Cerebral Cortex March 2015;25:772–787
doi:10.1093/cercor/bht274
Advance Access publication October 9, 2013

Cell Type-Specific Effects of Adenosine on Cortical Neurons

Karlijn I. van Aerde[1,4], Guanxiao Qi[1,2] and Dirk Feldmeyer[1,2,3]

[1]Forschungszentrum Jülich, Institute of Neuroscience and Medicine, INM-2, D-52425 Jülich, Germany, [2]Department of Psychiatry, Psychotherapy and Psychosomatics, RWTH Aachen University, Medical School, D-52074 Aachen, Germany, [3]JARA—Translational Brain Medicine, Aachen, Germany, [4]Current address: Netherlands Institute for Neuroscience, Royal Netherlands Academy of Arts and Science, 1105 BA Amsterdam, The Netherlands

Address correspondence to Dirk Feldmeyer, Forschungszentrum Jülich, Institute of Neuroscience and Medicine, INM-2, Leo-Brandt-Straße, Jülich D-52425, Germany. Email: d.feldmeyer@fz-juelich.de

The neuromodulator adenosine is widely considered to be a key regulator of sleep homeostasis and an indicator of sleep need. Although the effect of adenosine on subcortical areas has been previously described, the effects on cortical neurons have not been addressed systematically to date. To that purpose, we performed in vitro whole-cell patch-clamp recordings and biocytin staining of pyramidal neurons and interneurons throughout all layers of rat prefrontal and somatosensory cortex, followed by morphological analysis. We found that adenosine, via the A_1 receptor, exerts differential effects depending on neuronal cell type and laminar location. Interneurons and pyramidal neurons in layer 2 and a subpopulation of layer 3 pyramidal neurons that displayed regular spiking were insensitive to adenosine application, whereas other pyramidal cells in layers 3–6 were hyperpolarized (range 1.2–10.8 mV). Broad tufted pyramidal neurons with little spike adaptation showed a small adenosine response, whereas slender tufted pyramidal neurons with substantial adaptation showed a bigger response. These studies of the action of adenosine at the postsynaptic level may contribute to the understanding of the changes in cortical circuit functioning that take place between sleep and awakening.

Keywords: adenosine, cortical layers, heterogeneity, prefrontal cortex, rat

Introduction

Sleep is necessary for normal brain function, and biological clocks drive the sleep–waking cycle in a 24-h rhythm. However, sleep onset, duration, and intensity vary based on need. The neuromodulator adenosine is widely considered to be a key regulator of sleep homeostasis (Porkka-Heiskanen et al. 1997; Basheer et al. 2004) and is ubiquitously present in the cerebrospinal fluid at estimated concentrations of about 25 nM to 25 μM (Dunwiddie and Masino 2001; Kerr et al. 2013). Adenosine is a product of the ectoATPase-mediated metabolism of previously released ATP or can also be directly released by vesicular exocytosis as has been shown recently for parallel fibers in the cerebellum (Dunwiddie and Masino 2001; Klyuch et al. 2011, 2012; Schmitt et al. 2012). Adenosine is removed from the extracellular space by facilitated diffusion or active transport into neurons and glia, where it is phosphorylated by the enzyme adenosine kinase to form AMP (Dunwiddie and Masino 2001; Wall et al. 2007; Diogenes et al. 2012). The extracellular concentration of adenosine is approximately 15–20% higher during wakefulness than during sleep in a wide variety of brain areas and increases by approximately 40% after several hours of sleep deprivation (Huston et al. 1996; Porkka-Heiskanen et al. 2000; Basheer et al. 2004; Kalinchuk et al. 2011; Schmitt et al. 2012). When the adenosine tone was estimated at different times of day, a 4- to 5-fold difference was reported (Schmitt et al. 2012). Because of this, adenosine is often referred to as an endogenous "sleep factor" that reflects "sleep need." Interestingly, the increase in adenosine levels induced by sleep deprivation is specific for the basal forebrain, hippocampus, and neocortex and does not occur in the thalamus, hypothalamus, and brainstem (Huston et al. 1996; Porkka-Heiskanen et al. 2000). Several studies indicate that local administration of adenosine or adenosine receptor antagonists leads to changes in sleep–wake regulation (Basheer et al. 2004; Van Dort et al. 2009). Moreover, the pharmacological blockade of adenosine A_1 receptor function and the blockade of ATP release from astrocytes can prevent the cognitive deficits seen after sleep deprivation (Halassa et al. 2009; Florian et al. 2011).

In addition to its role in sleep homeostasis, adenosine is known for its neuroprotective effects and plays an important role in limiting tissue damage after stroke (Liang and Jacobson 1999; Yellon and Downey 2003) as well as in the prevention and suppression of epileptic seizures (Boison 2011).Adenosine has also been described to mediate the cognitive deficits of opiates and has been linked to other substances of abuse such as alcohol (Dunwiddie and Masino 2001; Lu et al. 2010; Ruby et al. 2010).

The predominant effect of adenosine is a general inhibition of neuronal activity (Segal 1982; Haas and Greene 1984; Dunwiddie and Fredholm 1989; Yoon and Rothman 1991; Prince and Stevens 1992; Dunwiddie and Masino 2001; Arrigoni et al. 2006; Fontanez and Porter 2006). This inhibition can be blocked by the application of an antagonist, the most well known of which is caffeine, an alkaloid present in coffee. Caffeine acts as an antagonist of the adenosine A_1 and A_{2A} receptors and increases the excitability of neurons as well as boosting arousal. The inhibition of neuronal activity through the G-protein-coupled adenosine A_1 receptor results from a hyperpolarization of the resting membrane potential (RMP) and a decrease in cellular input resistance through the opening of inward rectifying potassium (K_{ir}) channels on the postsynaptic site resulting in the shunting of synaptic inputs, and a decrease in release probability at the presynaptic site (Gerber et al. 1989; Thompson et al. 1992; Rainnie et al. 1994; Cunha 2001). In addition, adenosine can inhibit hyperpolarization-activated cyclic nucleotide (HCN)-gated channels by decreasing cAMP levels through the adenosine A_1 receptor, leading to a further hyperpolarization of the membrane potential (Rainnie et al. 1994; Arrigoni et al. 2006).

Adenosine A_1 and A_{2A} receptors are coupled with different types of G-protein receptors: G_i and G_s, respectively, and can therefore exert distinct effects (Cunha 2001; Dunwiddie and Masino 2001). Adenosine A_1 receptors are widely expressed, including the prefrontal and somatosensory cortex (Elmenhorst et al. 2007; Van Dort et al. 2009), whereas high adenosine A_{2A}

receptor expression is restricted to the striatum and olfactory tubercle (Cunha 2001; Dunwiddie and Masino 2001). However, adenosine A_{2A} receptors can exert stimulatory effects on the hippocampus and neocortex (Rebola et al. 2008; Van Dort et al. 2009), which of the effects prevails depends not only on receptor expression patterns but also on the adenosine concentration, because the adenosine A_1 receptors have a much higher affinity for adenosine compared with adenosine A_{2A} receptors (Dunwiddie and Masino 2001). Adenosine A_{2B} and A_3 receptors have also been reported, both displaying a very low-adenosine affinity (Dunwiddie and Masino 2001).

Several studies point to an important role of the prefrontal cortex in sleep homeostasis and suggest that adenosine might act in the prefrontal cortex to alter cognition (Huber et al. 2000; Muzur et al. 2002; Van Dort et al. 2009; Mander et al. 2013). Interestingly, deprivation of only one night of sleep increases adenosine A_1 receptor binding in the frontal cortex in human (Elmenhorst et al. 2007) and in cortical regions in rat (Elmenhorst et al. 2009). Moreover, many clinical features of sleep deprivation are associated with a general dysfunction of the prefrontal cortex (Muzur et al. 2002). These include not only cognitive deficits such as attention loss and decreased working memory but also increased irritability and apathy (Harrison et al. 2000).

Cortical processing depends on the interaction between distinct neuronal types in different cortical layers. Pyramidal neurons in the main output layer of the neocortex, layer 5, have been extensively studied at the electrophysiological and morphological level. These studies have revealed differences in subcortical projection areas of different pyramidal cell subtypes as well as differences in intralaminar connections, suggesting that pyramidal cells can form subnetworks depending on the cell type (Molnar and Cheung 2006; Wang et al. 2006; Otsuka and Kawaguchi 2008; Dembrow et al. 2010; Hirai et al. 2012). Additionally, pyramidal cell subtypes, like interneurons, are differentially affected by neuromodulators such as acetylcholine, noradrenaline, serotonin, and dopamine (Beique et al. 2007; Couey et al. 2007; Eggermann and Feldmeyer 2009; Dembrow et al. 2010; Gee et al. 2012; Poorthuis et al. 2013). To examine the impact of adenosine on individual neurons in the cortex, we studied the effects of adenosine on neuronal properties in the rat prefrontal and somatosensory cortex. We made whole-cell patch-clamp recordings from pyramidal neurons and interneurons throughout the cortical layers. Post hoc staining of the labeled neurons, in conjunction with the electrophysiological data, allowed us to identify interneurons and several pyramidal subtypes within each cortical layer (Van Aerde and Feldmeyer 2013). We found that adenosine exerts differential effects depending on neuronal cell type and laminar location. Some neurons, such as interneurons and pyramidal neurons, in layer 2 and a subpopulation of L3 pyramidal neurons were insensitive to adenosine modulation, whereas other pyramidal cells in layers 3–6 were hyperpolarized to varying degrees. The present results of the action of adenosine at the postsynaptic level may contribute to the understanding of the changes in cortical circuit functioning that take place between sleep and wake states.

Materials and Methods

Slice Preparation

All experimental procedures were performed in accordance with the German Animal Welfare Act, the European Directive on the Protection of Animals used for Scientific Purposes, and the guidelines of the Federation of European Laboratory Animal Science Association.

Wistar rats (Charles River, either sex) aged 24–46 postnatal days (P24–46) were anesthetized with isoflurane and decapitated, and their brains were quickly removed, while being placed in ice-cold artificial cerebrospinal fluid (ACSF) containing: 125 mM NaCl, 2.5 mM KCl, 1.25 mM NaH_2PO_4, 5 mM $MgSO_4$, 1 mM $CaCl_2$, 25 mM $NaHCO_3$, 25 mM glucose, 3 mM Myo-Inositol, 2 mM Na-pyruvate, and 0.4 mM vitamin C (300 mOsm). Animals were sacrificed approximately 2–3 h after the beginning of the light period.

For prefrontal cortex slices, coronal sections (350 µm) of the prelimbic medial prefrontal cortex were cut, whereas for somatosensory cortex oblique coronal slices (300–350 µm) of the somatosensory cortex were cut at 45° to the midline (modified from Agmon and Connors 1992) in ice-cold ACSF bubbled with carbogen gas (95% O_2/5% CO_2) using a MICROM vibratome slicer (Walldorf, Germany). For older animals (>P35), a sucrose-based slicing solution was used containing: 206 mM sucrose, 2.5 mM KCl, 1.25 mM NaH_2PO_4, 3 mM $MgSO_4$, 1 mM $CaCl_2$, 25 mM $NaHCO_3$, and 25 mM glucose (300 mOsm).

Slices were then transferred to a holding chamber placed in a water bath at 35 °C and left to recover for at least 1 h, thereafter the water bath was allowed to cool down to room temperature. Slices were stored for up to 8 h in ACSF containing: 125 mM NaCl, 2.5 mM KCl, 1.25 mM NaH_2PO_4, 1 mM $MgSO_4$, 2 mM $CaCl_2$, 25 mM $NaHCO_3$, and 25 mM glucose, bubbled with carbogen gas (95% O_2/5% CO_2).

Electrophysiology

Pyramidal cells and interneurons, visualized using infrared differential interference contrast (DIC) microscopy, were selected on the basis of their morphology and firing pattern. All experiments were performed at 30 ± 1 °C. The subphysiological recording temperature was chosen to limit the decrease in oxygenation at higher temperatures. Basic passive and active cell properties were assessed by initial hyperpolarization, followed by stepped depolarization.

Recordings were made using an EPC10 amplifier (HEKA, Lambrecht, Germany), sampled at 10 kHz, and filtered at 2.9 kHz using the Patchmaster software (HEKA), and later analyzed off-line (Igor Pro software, Wavemetrics, Lake Oswego, OR, USA).

Patch pipettes (4–8 MΩ) were pulled from thick-wall borosilicate capillaries (outer diameter: 2 mm; inner diameter: 1 mm) and were filled with intracellular solution containing 135 mM K-gluconate, 4 mM KCl, 10 mM HEPES, 10 mM Na-phosphocreatine, and 4 mM ATP-Mg and 0.3 mM GTP-Na (pH adjusted to 7.3 with KOH; osmolarity, ~300 mOsm). Biocytin at a concentration of 3–5 mg/mL was added to the internal solution. In a subset of experiments, 50 µM ZD7288 was added to the intracellular solution from a 5-mM stock solution.

Whole-cell series resistance was on average 31.0 ± 9.8 MΩ (mean ± standard deviation, $n = 110$) and was compensated by 80%. Neurons were excluded from the analysis when their series resistance was above 50 MΩ or changed by more than 25% during the experiment.

Drugs and Chemicals

Adenosine, barium chloride, 8-cyclopentyl-1,3-dimethylxanthine (CPT), and biocytin were from Sigma-Aldrich (Steinheim, Germany); N^6-cyclopentyladenosine (CPA) and ZD7288 from Tocris (Bristol, UK).

Histological Procedures

After intracellular recording, the slices were fixed in 4% paraformaldehyde in 0.1 M phosphate buffer (PB; pH 7.4) for at least 24 h, followed by several rinses with PB. Subsequently, slices were treated with 1% H_2O_2 in PB for 10 min to reduce endogenous peroxidase activity. Biocytin-filled cells were visualized using an avidin-biotinylated horseradish peroxidase complex reaction (ABC-Elite; Camon, Wiesbaden, Germany) with 3,3′-diaminobenzidine (Sigma-Aldrich, St. Louis, MO, USA) as a chromogen giving a dark reaction product. After dehydration and embedding in Moviol (Clariant, Sulzbach, Germany) or embedding in Eukitt (Marienfeld Laboratory, Glassware, Lauda-Königshof, Germany), neurons were reconstructed using the Neurolucida software

(MBF Bioscience) at ×400–×630 (Radnikow et al. 2012; Marx et al. 2012).

Data Analysis

Electrophysiological data were analyzed using custom-written procedures in Igor Pro 6.0 (Wavemetrics).

Passive Cell Properties and Spike-Time Adaptation

The input resistance (R_{in}) was calculated as the slope of the linear fit between −60 and −70 mV of the current–voltage (*IV*) relationship. The membrane time constant (τ_m) was estimated with a mono-exponential fit of the voltage response after a current step of −50 pA. Rheobase current, the minimal current that elicited an action potential (AP), was determined using a small step size of 10 pA. I_h current was activated by changing the holding potential of −60 mV through a range of test potentials in −10 mV steps. I_h was calculated as the difference between the minimum current (measured within 100 ms) and sustained response.

Spike-time adaptation is shown for the current step when at least 10 APs were elicited. We took the approach of comparing neurons with approximately the same number of APs instead of the response to the same amount of current injection, because individual differences in rheobase current and R_{in} would lead to a highly variable number of elicited APs with a fixed current injection. Although spike-time adaptation was similar for individual neurons for current steps that elicited more than approximately 7 APs, especially the first interspike-interval (ISI) was variable for lower current injections when <7 APs were elicited.

Adenosine Application

Because adenosine could be washed out completely within 5–10 min, and the membrane potential before wash-in of adenosine and after wash-out were comparable (L3 pyramidal neurons, $n = 6$, $P = 0.77$), it was possible to use the wash-out as an indicator of the adenosine effect on experiments in which adenosine was applied during a whole-cell voltage clamp and wash-out was measured in current-clamp configuration. This conversion was used to combine the voltage and current-clamp experiments of L3 pyramidal neurons.

Morphology

Neurons were 3-dimensionally reconstructed using the Neurolucida® software (MBF Bioscience). The field span of apical and basal dendrites was defined as the widest distance between, respectively, apical and basal dendrites, measured parallel to the surface. Other morphological parameters like the total dendritic length, number of branches, and soma size were analyzed with the Neuroexplorer® software (MBF Bioscience). The soma size was calculated as the maximal soma circumference from the projection in the 2D plane.

Definition of Cortical Layers

The definition of cortical layers in the medial prefrontal cortex (mPFC) is described in great detail in our accompanying study (Van Aerde and Feldmeyer 2013). In short, layer borders were drawn under low-magnification conditions using maximal contrast. The embedding of slices in Eukitt (see above) prevented fading of cytoarchitectural features and improved the contrast between layers considerably (Marx et al. 2012). Layer borders were defined based on cytoarchitectural features of which cell density and cell soma size were most important in agreement with earlier studies of the prefrontal cortex (Van Eden and Uylings 1985; Gabbott et al. 1997, 2005). In the somatosensory cortex, granular layer 4 can be seen as a darker band with barrel-like structures. Layer 2/3 is situated supragranular, and layer 5 is situated subgranular. Sublamina 5A and 5B can be easily distinguished in fixed slices: Sublamina 5A is bordered between the darker layers 4 and 5B (see inset in Fig. 7*A*).

Cluster Analysis and Statistics

Data are represented as mean ± standard error of the mean. Statistical analysis used paired or unpaired Student's *t*-test or analysis of variance (ANOVA) test for multiple comparisons, followed by a post hoc Tukey test or a Student Newman–Keuls test when >3 groups were compared. Correlation analysis was performed calculating Pearson correlation coefficients.

Pyramidal neurons were classified as described in Van Aerde and Feldmeyer (2013). In short, unsupervised cluster analysis (CA) was performed using physiological and morphological parameters. Physiological parameters used were: Ratio of ISI_1/ISI_9, ISI_2/ISI_9, ISI_3/ISI_9, RMP, R_{in}, τ_m, rheobase, and voltage sag. Morphological parameters included: Field span of apical and basal dendrites, total length of apical and basal dendrites, number of branches of apical and basal dendrites, and vertical span of the apical dendrite for L6 pyramidal neurons. The final number of clusters was suggested by the Thorndike procedure, where the maximal derivative of the sorted linkage distances was taken as the cut-off value (Thorndike 1953). Each parameter was normalized as min–max normalization. Principal component analysis (PCA) was used to eliminate correlated variables to avoid double weighting or misinterpretation of the CA. Parameters that were often, but not always, contributing in a similar way to the PCA were the ratio of ISI_1/ISI_9 and ISI_2/ISI_9. Morphological parameters that were often correlated were the total length and number of branches of apical or basal dendrites. Using this approach we were able to exclude all parameters that were highly correlated from the CA. To eliminate uninformative parameters, the resulting groups or clusters of the CA were then compared for each parameter using ANOVA tests, and the CA was repeated with only those parameters included that showed significant different values between the groups.

All statistical tests were performed with the XLSTAT software (Addinsoft, Andernach, Germany). Single and double asterisks represent $P < 0.05$ and <0.01, respectively.

Results

To study the effect of adenosine on different neuronal cell types, we recorded from 68 pyramidal neurons and 19 interneurons located throughout the cortical layers (L) 2–6 of the rat prelimbic cortex, which is part of the mPFC. The prelimbic cortex is situated along the midline of the cortex and is bordered by the anterior cingulate cortex and the infralimbic cortex (Paxinos and Watson 2005). In addition, we recorded from 19 pyramidal neurons and 4 interneurons in layers 2 and 5 in the "barrel" field of the rat somatosensory cortex. In the accompanying manuscript, we have classified pyramidal neurons of the mPFC in several subtypes (Van Aerde and Feldmeyer 2013). In this same set of cells, we also studied the effects of adenosine. Adenosine was bath-applied for 5–10 min, and the effect on the electrophysiological properties of the neuron was continuously recorded. After the electrophysiological recordings, slices were fixed and processed for staining, and neurons were reconstructed to analyze their morphology. Only neurons with stable RMPs below −60 mV and with excellent staining of soma and dendrites were used for the analysis of the neuron-specific adenosine effects.

To verify if adenosine acts mainly through the adenosine A_1 receptor in the mPFC, we first made recordings from L5 pyramidal neurons and bath-applied adenosine and A_1 specific agonists and antagonists. Bath application of 100 μM adenosine led on average to a 3.8 ± 0.3 mV hyperpolarization of the RMP of L5 pyramidal neurons ($n = 30$; Fig. 1*A* and Table 1). The size of the hyperpolarization was dependent on the adenosine concentration (Fig. 1*B*, EC_{50} 18.6 ± 4.3 μM, $n = 8$), but bath application of 5 μM adenosine already caused a significant hyperpolarization [Fig. 1*B*, RMP: −66.1 ± 1.2 mV (control), −67.3 ± 1.2 mV (5 μM adenosine), difference −1.2 ± 0.4 mV, $n = 10$, paired *t*-test $P < 0.01$]. The effect of adenosine could be mimicked by bath application of 1 μM CPA, a specific agonist of the adenosine A_1

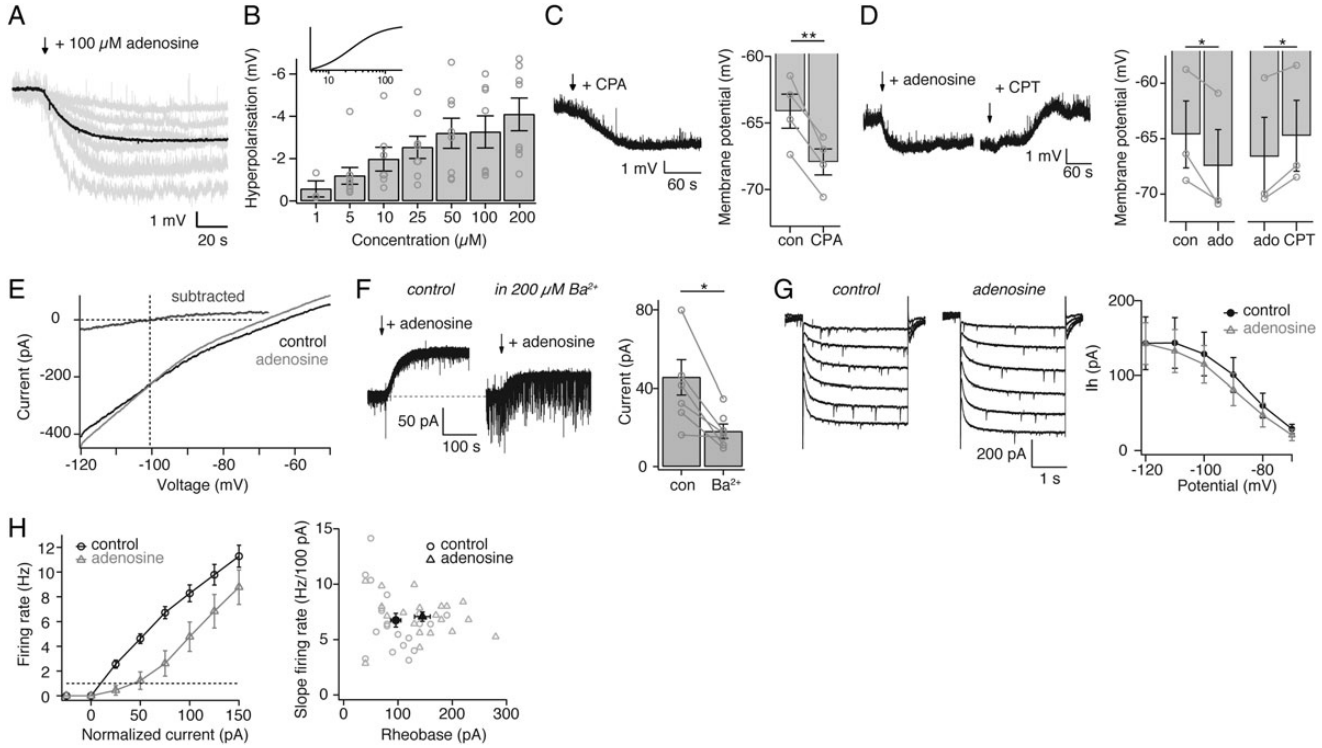

Figure 1. Adenosine hyperpolarizes the membrane potential of L5 pyramidal cells through the adenosine A_1 receptor. (*A*) Example traces of the RMP during bath application of 100 μM adenosine (start at arrow). Average response is shown in black ($n = 34$). (*B*) Example dose–response plot (inset) and average responses for adenosine concentrations from 1 to 200 μM ($n = 6$). (*C*) Example trace (left) and average response (right, $n = 4$) of the RMP during application of 1 μM adenosine A_1 receptor agonist CPA. (*D*) Example trace (left) and average response (right, $n = 3$) of the RMP during application of 100 μM adenosine, followed by coapplication of 1 μM the A1R antagonist CPT. (*E*) Example *IV* plot during the absence (control) and presence of adenosine. Adenosine induced an outward current with a reversal potential of −99.8 mV. (*F*) Example trace (left) and average responses (right, $n = 6$) from L5 pyramidal neurons held at −60 mV in whole-cell voltage-clamp configuration during application of 100 μM adenosine, in the absence (left, control) or presence of 200 μM Ba^{2+}. (*G*) Example traces and average responses (right, $n = 6$) from L5 pyramidal neurons held at varying hyperpolarizing holding potentials (−60 to −120 mV) to measure the I_h current before (left) and during (middle) application of 100 μM adenosine. Note that experiments were performed in the presence of 200 μM Barium. (*H*) Left, firing rate as a function of injected current before (circles) and after (triangles) adenosine application. Note that the current is normalized to the rheobase current of the control condition. Right, slope of the firing rate as a function of current plotted against rheobase. Rheobase current was calculated from 10 pA current steps. Averages for the control (circles) and adenosine (triangles) condition are shown with error bars. $^*P < 0.05$, $^{**}P < 0.01$.

Table 1
Adenosine modulation of passive properties of pyramidal neurons in the prefrontal cortex

	Control	100 μM Adenosine	Wash	*P*
Layer 2 pyramidal neurons ($n = 8$)				
RMP (mV)	−76.5 ± 1.5	−76.4 ± 1.3	−77.0 ± 1.3	0.73
Input resistance (MΩ)	160 ± 14	173 ± 17	164 ± 16 ($n = 7$)	<0.01/0.58
Time constant (ms)	20.5 ± 1.4	23.4 ± 1.2	24.9 ± 1.7 ($n = 7$)	0.07/0.37
Rheobase (pA)	186 ± 12	188 ± 13	191 ± 14 ($n = 7$)	0.86
Layer 3 pyramidal neurons				
Responding ($n = 8$)				
RMP (mV)	−67.5 ± 0.8	−70.9 ± 0.8	−67.6 ± 1.0	<0.01/<0.01
Input resistance (MΩ)	138 ± 11	116 ± 11	140 ± 11	0.02/<0.01
Time constant (ms)	29.3 ± 2.9	24.6 ± 2.0	29.3 ± 3.4	0.056/0.18
Rheobase (pA)	124 ± 11	175 ± 18	119 ± 10	0.01/<0.01
Nonresponding ($n = 4$)				
RMP (mV)	−78.9 ± 1.3	−79.2 ± 1.4	−79.7 ± 1.6	0.23
Input resistance (MΩ)	142 ± 16	150 ± 18	150 ± 14	0.04/0.96
Time constant (ms)	18.5 ± 0.7	17.2 ± 1.9	19.7 ± 3.3	0.41
Rheobase (pA)	233 ± 15	228 ± 26	230 ± 11	0.70
Layer 5 pyramidal neurons ($n = 20$)				
RMP (mV)	−64.6 ± 0.5 ($n = 30$)	−68.4 ± 0.6 ($n = 30$)	−64.3 ± 0.6 ($n = 28$)	<0.01/<0.01
Input resistance (MΩ)	208 ± 25	178 ± 24	224 ± 31	<0.01/<0.01
Time constant (ms)	35.0 ± 1.9 ($n = 18$)	28.4 ± 1.6 ($n = 18$)	38.6 ± 2.7 ($n = 18$)	<0.01/<0.01
Rheobase (pA)	96 ± 9	145 ± 14	90 ± 10	<0.01/<0.01
Layer 6 pyramidal neurons ($n = 6$)				
RMP (mV)	−70.1 ± 1.9 ($n = 10$)	−74.4 ± 1.8 ($n = 10$)	−67.3 ± 1.5 ($n = 8$)	<0.01/<0.01
Input resistance (MΩ)	301 ± 46	272 ± 40	400 ± 77 ($n = 5$)	0.31/0.03
Time constant (ms)	26.1 ± 4.0	20.7 ± 2.2	40.2 ± 5.0 ($n = 5$)	0.21/0.02
Rheobase (pA)	93 ± 22	120 ± 19	54 ± 14 ($n = 5$)	0.10/<0.01

Note: Average ± SEM; RMP, resting membrane potential. *P* lists the results from paired *t*-tests between control and adenosine. When $P < 0.10$ the result from the paired *t*-test between adenosine and wash-out is also given. The number of cells for the calculation of passive properties is generally lower than for the RMP to allow an uninterrupted continuous recording of the RMP in a subset of experiments.

receptor [Fig. 1*C*, RMP: −64.1 ± 1.3 mV (control), −67.9 ± 1.0 mV (CPA), difference −3.8 ± 0.6 mV, $n = 4$, paired *t*-test $P < 0.01$]. In addition, bath application of the adenosine A_1 receptor antagonist CPT reversed the adenosine-induced hyperpolarization to baseline levels [Fig. 1*D*, RMP: −64.6 ± 3.0 mV (control), −66.6 ± 3.4 mV (adenosine), −64.7 ± 3.2 mV (adenosine + 1 μM CPT), $n = 3$, paired *t*-test $P < 0.05$].

The application of adenosine induced an outward current with a reversal potential of −103.8 ± 2.9 mV ($n = 5$) that is close to the equilibrium potential of potassium ($E_{K+,rev}$, −105 mV; Fig. 1*E*). The outward current that was elicited by adenosine was reduced when barium was present in the perfusion solution (Fig. 1*F*). In a subset of experiments, we also included ZD7288 in the intracellular solution to block possible actions of adenosine on HCN channels (see below). However, as the inclusion of ZD7288 did not lead to different results, we grouped the results. The reversal potential of the adenosine-induced current and the reduction in the presence of barium suggest that the previously described actions of the adenosine A_1 receptor on inward rectifying potassium channels also apply to prefrontal cortex pyramidal neurons (Haas and Greene 1984; Greene and Haas 1985; Mccormick and Williamson 1989; Cunha 2001; Dunwiddie and Masino 2001).

HCN-gated channels can be modulated by adenosine via inhibition of adenylate cyclase through the G_i-protein complex coupled with the adenosine A_1 receptor. Activation of A_1 receptors will lead to a decrease in intracellular cAMP levels and hence, a reduced open probability of HCN channels (Basheer et al. 2004; Li et al. 2011). This would lead to a decreased inward current for cations resulting in a hyperpolarization of the membrane potential. To investigate a possible effect of adenosine on the opening of HCN channels, we measured I_h currents in a subset of cells in the presence of 200 μM barium. From these experiments, no clear effect on I_h current could be observed (Fig. 1*G*).

Adenosine application affected the passive properties of L5 pyramidal neurons: The cellular input resistance and the membrane time constant decreased, which can be explained by the increased amount of open (potassium) channels (Table 1). The firing rate as a function of injected current (*F:I* plot) was shifted after adenosine application, suggesting a change in cellular excitability under conditions of high adenosine levels (Fig. 1*H*). Cellular excitability was more precisely determined by measurement of the rheobase current, the minimal current that elicited an AP, in 10 pA steps (see Materials and Methods). The rheobase current was significantly and reversibly increased after adenosine application, indicating that adenosine reduces cellular excitability (Fig. 1*H* and Table 1).

Next, we studied the effect of adenosine on different pyramidal subtypes in the rat mPFC.

Layer 2 Pyramidal Neurons Are Insensitive to Adenosine

In the rat mPFC, layer 2 is clearly distinguishable from layer 3 as a thin dark band that is densely packed with neuron somata; it is located directly beneath layer 1 (Fig. 2*A*). Layer 2 is the thinnest layer of the prefrontal cortex containing only a few "rows" of pyramidal neurons. On a qualitative level, the density of neuron somata is lower in layer 3 than in layer 2 as can be seen at both the microscopic and macroscopic levels (Fig. 2*A*). Morphologically, L2 pyramidal neurons differ from L3 pyramidal neurons in the field span of their apical and basal dendrites: The apical dendritic tree of L2 pyramidal neurons has typically a much larger field span than the basal dendritic tree, whereas this ratio is smaller or reversed for L3 pyramidal neurons (Fig. 2*B*, see accompanying paper for more details; Van Aerde and Feldmeyer 2013).

Pyramidal neurons in layer 2 did not show a change in the RMP in response to adenosine application (Fig. 2*C* and Table 1). Also, passive cell properties, such as the rheobase (minimal current to elicit an AP) and the membrane time constant, were unchanged (Table 1).

Layer 3 Contains Adenosine-Sensitive and -Insensitive Pyramidal Neurons

Pyramidal cells in layer 3 of the prefrontal cortex showed a high variability in response to adenosine application: About 70% of the population responded with a hyperpolarization of the RMP following adenosine application, whereas the remaining 30% was insensitive to adenosine application (Fig. 3*A*). Passive cell properties showed significant changes for the adenosine-sensitive neurons, but remained unchanged for the adenosine-insensitive L3 pyramidal neurons (Table 1).

To ensure that we had correctly targeted L3 and not L2 pyramidal neurons, we performed post hoc morphological analysis. Both the ratio of the apical to the basal dendritic field span and the total length of basal dendrites differed significantly between L2 pyramidal neurons and nonresponding L3 neurons [ratio of the apical/basal dendritic field span, 1.7 ± 0.1 (L2, $n = 8$), 1.0 ± 0.03 (L3 nonresponding, $n = 6$), $P < 0.001$; total length

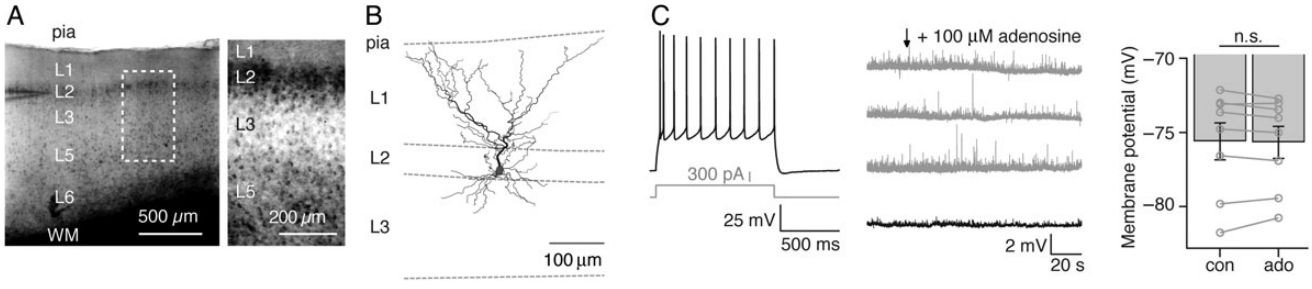

Figure 2. Adenosine does not modulate L2 pyramidal neurons. (*A*) Left, DIC image at low magnification where pia, successive layers (L), and white matter (WM) are indicated. Note the patch pipette in left layer 2. Right, DIC image from another brain slice at higher magnification (comparable with the boxed region at the left), where layers can be particularly well recognized. (*B*) Morphological reconstruction of soma and dendrites from a L2 pyramidal neuron. Note the large field span of apical dendrites compared with basal dendrites. Right, electrophysiological profile: The response is shown when minimally 10 APs were elicited with the corresponding current step in gray. (*C*) Left, example traces of the RMP during bath application of 100 μM adenosine (start at arrow). Average response is shown in black ($n = 8$). Right, average RMP during control ("con") and adenosine ("ado") conditions ($n = 8$, $P = 0.73$).

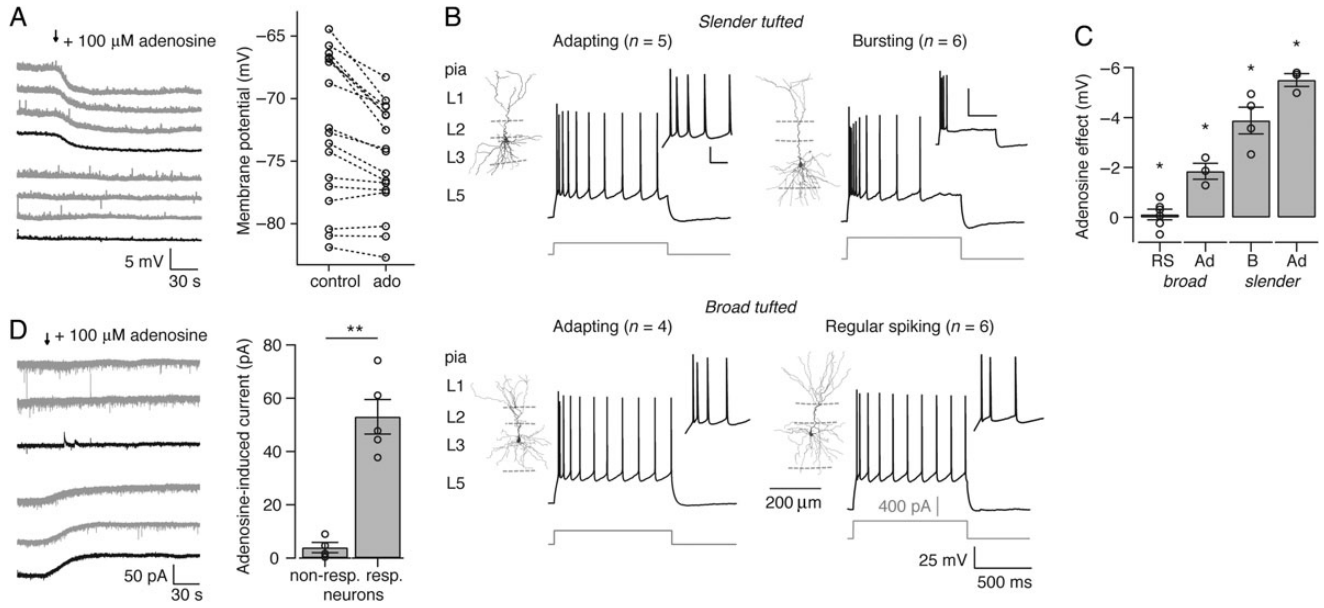

Figure 3. Layer 3 contains adenosine-sensitive and -insensitive pyramidal neurons. (*A*) Left, example traces of the RMP during bath application of 100 µM adenosine (start at arrow). Average response is shown in black (top, responding neurons; bottom, nonresponding neurons). Right, RMP during control and 100 µM adenosine ("ado") conditions. (*B*) Morphological reconstruction of soma and dendrites and corresponding electrophysiological profile from L3 pyramidal cell subtypes. The electrophysiological response is shown when minimally 10 APs were elicited (corresponding current steps in gray). The inset shows a magnification of the first spikes (scale bar: 25 mV, 50 ms), except for bursting neurons. Here, the inset shows the typical response to medium current injections: a burst of 4–5 APs followed by silence (scale bar: 50 mV, 500 ms). (*C*) Adenosine-induced hyperpolarization of the RMP [RS, $n = 6$; broad tufted adapting (Ad), $n = 3$; B, bursting, $n = 4$; slender tufted Ad, $n = 3$]. (*D*) Left, example traces of the current across the cell membrane during bath application of 100 µM adenosine (start at arrow) when the neurons were voltage clamped at −50 mV. Average response is shown in black (top, nonresponding neurons; bottom, responding neurons). Right, adenosine-induced current in nonresponding ("nonresp.", $n = 4$) and responding neurons ("resp.", $n = 5$). $^*P < 0.05$, $^{**}P < 0.01$.

basal dendrites, 1660 ± 197 µm (L2, $n = 8$), 2901 ± 243 µm (L3 nonresponding, $n = 6$), $P < 0.01$].

We have previously classified layer 3 pyramidal neurons into 4 pyramidal subtypes based on morphological and electrophysiological parameters: (1) Broad tufted regular spiking (RS) neurons that responded upon current stimulation with regular firing, except for the first ISI, adapting neurons with slender (2) or broad (3) tufted morphologies that would display more adaptation in their spike timing, and (4) slender tufted bursting neurons that responded with bursts of APs upon electrical stimulation. This bursting behavior was not seen in pyramidal neurons from any other layer of the prefrontal cortex (Van Aerde and Feldmeyer 2013; Fig. 3*B*).

The 4 subtypes of L3 pyramidal neurons differed in their sensitivity for adenosine: While bursting and adapting neurons showed varying hyperpolarizing responses in the range of 1.3–5.8 mV, all nonresponding L3 neurons belonged to the RS subtype (Fig. 3*B*,*C*). Adenosine-sensitive L3 neuron subtypes differ with respect to the mean amplitude of the adenosine-induced hyperpolarization: Slender tufted adapting L3 neurons showed on average the largest response to adenosine, followed by bursting L3 neurons. Broad tufted adapting L3 neurons showed the smallest response of the adenosine-sensitive L3 neurons (ANOVA $P < 0.01$, followed by post hoc Tukey test $P < 0.05$).

An RMP of both nonresponding L2 and RS L3 pyramidal neurons was more hyperpolarized, and therefore closer to the equilibrium potential of potassium ($E_{K+,rev}$, −105 mV), than that of the responding L3 neurons (Figs 1*C* and 2*A*). Because this could potentially bias our results, we performed additional experiments in L2 and L3 pyramidal neurons in which the membrane potential was voltage clamped at −50 mV. This should ensure that if adenosine had an effect on K^+ channel opening, it would be clearly visible as an increased outward current. In addition, we encountered both responding neurons and nonresponding neurons [Fig. 2*D*, $I_{-50\ mV}$ nonresponders 175 ± 9 pA (control), 179 ± 8 pA (adenosine), difference 4 ± 2 pA, $n = 4$ ($n = 2$ in L2 and $n = 2$ in L3), $P = 0.13$; responders 177 ± 30 pA (control), 230 ± 35 pA (adenosine), difference 53 ± 6 pA, $n = 5$ (in L3), $P < 0.01$].

Furthermore, RS pyramidal neurons in layer 3 differed greatly from the other L3 pyramidal neuron subtypes with respect to their passive electrical properties. Most strikingly, these neurons had extremely high rheobase values, indicating a fundamental difference in neuronal excitability between the subpopulations (Van Aerde and Feldmeyer 2013).

Size of Adenosine Response Depends on Pyramidal Cell Type in Layer 5

All L5 pyramidal neurons that we recorded showed a hyperpolarizing response following adenosine application, albeit to a different extent (Fig. 1*A*). Between L5 pyramidal neurons, the RMP was very similar with a small coefficient of variation (CV) of approximately 4%; in contrast, the amplitude of the hyperpolarization showed a markedly larger variation (CV = 46%; $n = 30$). Passive cell properties were also affected by adenosine application (Table 1). The rheobase current increased significantly illustrating the reduced excitability of L5 pyramidal neurons under conditions of high adenosine levels (Table 1).

L5 pyramidal neurons of the prefrontal cortex can be categorized according to their electrophysiological and morphological properties (Yang et al. 1996; Degenetais et al. 2002;

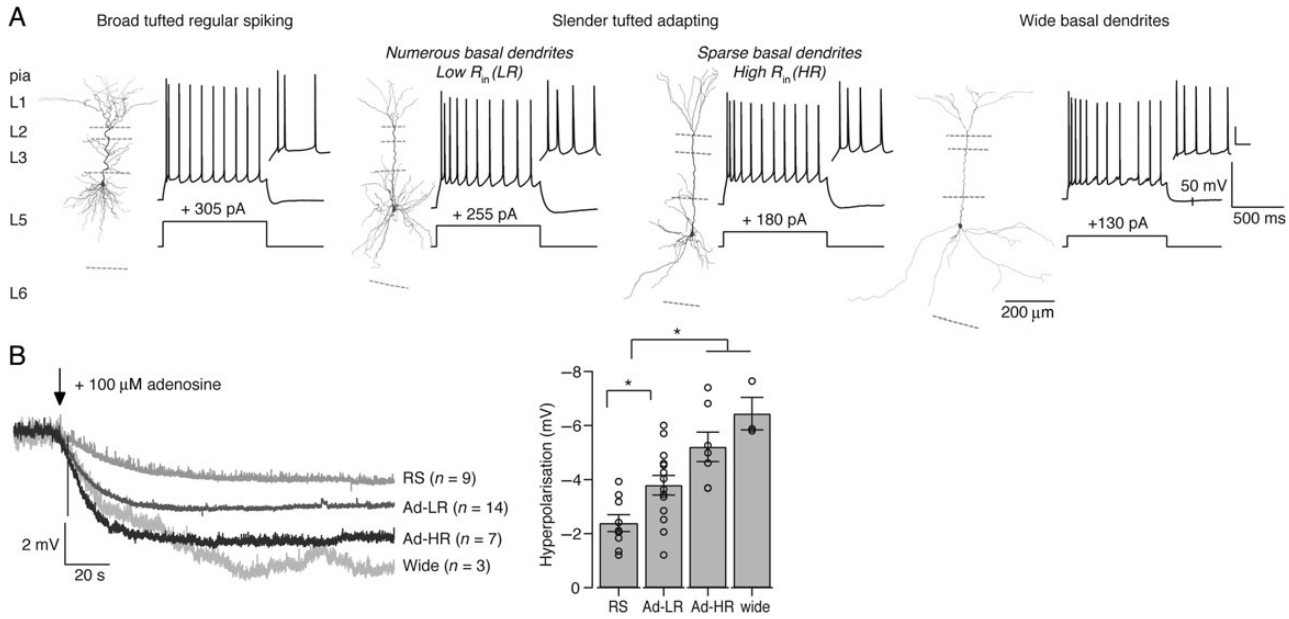

Figure 4. Response size depends on the subtype of layer 5 (L5) pyramidal cells. (*A*) Morphological reconstruction of soma and dendrites and corresponding electrophysiological profile from L5 pyramidal subtypes. Note that "wide" L5 neurons (right) were rare (~6% of total L5 neurons). The electrophysiological response is shown when minimally 10 APs were elicited with corresponding current steps below. The inset shows a magnification of the first 3–4 spikes (scale bar: 25 mV, 50 ms). (*B*) Left, average traces of the RMP during bath application of 100 µM adenosine (start at arrow) for the 4 L5 pyramidal subtypes. Right, adenosine-induced hyperpolarization of the RMP (RS, $n = 9$; Ad-LR, $n = 14$; Ad-HR, $n = 7$, wide, $n = 3$). *$P < 0.05$.

Wang et al. 2006; Chang and Luebke 2007). In addition, retrograde labeling studies show that specific electrophysiological cell types have distinct projection areas: RS neurons mainly project onto the thalamus and pontine nuclei in the brainstem, whereas neurons with adapting spike trains preferentially innervate the ipsi- and contralateral striatum or contralateral cortex (Dembrow et al. 2010; Gee et al. 2012). We have classified layer 5 pyramidal neurons into 4 groups: (1) Broad tufted RS neurons that show little adaptation, with the exception of the first ISI, a high threshold for firing, low-input resistance, and a short time constant; (2) slender tufted adapting neurons that show more adaptation have a low threshold for firing, high input resistance, and a long time constant ("adapting high-resistance neurons," Ad-HR), (3) slender tufted adapting neurons with intermediate values for input resistance, rheobase, and time constant ("adapting low-resistance neurons," Ad-LR), and finally, (4) pyramidal neurons that are characterized by a very wide field span of the basal dendrites ("wide" neurons). Note, however, that this last subtype is rare (~6% of L5 neurons; Fig. 4*A*; Van Aerde and Feldmeyer 2013).

In this same set of cells, we also tested for the effects of adenosine. Subtypes of L5 pyramidal neurons differed in the size of their response to adenosine application. Slender tufted Ad-HR and L5 wide neurons showed the largest hyperpolarizing responses of about 5–6 mV, whereas broad tufted RS pyramidal neurons showed on average the smallest response [Fig. 4*B*, adenosine-induced hyperpolarization: -2.4 ± 0.3 mV (RS, $n = 9$), -3.7 ± 0.5 mV (Ad-LR, $n = 14$), -5.2 ± 0.5 (Ad-HR, $n = 7$), -6.5 ± 0.6 mV (L5-wide, $n = 3$), ANOVA test $P < 0.01$, post hoc Tukey test $P < 0.01/0.05$].

Thus, pyramidal neurons in layer 5 of the prefrontal cortex showed a heterogeneous response to the neuromodulator adenosine. Neuronal subtypes displaying a more adaptive firing pattern were more sensitive to modulation by adenosine than regular firing pyramidal neurons.

Layer 6 Pyramidal Neurons Are All Sensitive for Adenosine

Layer 6 pyramidal neurons in the mPFC showed a great morphological variability. The diverse morphology of layer 6 neurons has been reported before for other brain areas (Tömböl 1984; Van Brederode and Snyder 1992; Thomson 2010; Marx and Feldmeyer 2012; Pichon et al. 2012). The mPFC has a high percentage (~35%) of "tall" L6 neurons with apical dendrites ascending to layer 1; a fraction of <5% has been reported for other cortical areas (Katz 1987; Van Brederode and Snyder 1992; Bailey et al. 2012; Van Aerde and Feldmeyer 2013).

All pyramidal neurons in layer 6 showed a hyperpolarizing response to adenosine application and a trend toward a decrease in cell excitability (Fig. 5*A* and Table 1).

We have previously classified layer 6 neurons into 2 main clusters: (1) Tall pyramidal neurons with apical dendrites extending into layer 1 ($n = 5$ or 33%) and (2) short L6 pyramidal neurons with apical dendrites confined to layers 3–6 ($n = 10$ or 67%). This last category could be subdivided into short L6 pyramidal neurons with a wider field span of basal dendrites ("short and broad," $n = 5$ or 33%) and L6 pyramidal neurons with more compact dendritic trees ("small," $n = 5$ or 33%; Van Aerde and Feldmeyer 2013). In this same set of cells, we also tested for the effects of adenosine. However, there was no significant difference in the size of the adenosine response for the different morphological subtypes (Fig. 5*C*).

To summarize, pyramidal neurons from different layers in the rat mPFC showed strong heterogeneity in their response to the neuromodulator adenosine: L2 pyramidal neurons and RS L3 neurons were insensitive to adenosine application, whereas adapting and bursting L3 neurons and pyramidal neurons in layers 5 and 6 showed hyperpolarizing responses of variable mean amplitude (Fig. 6).

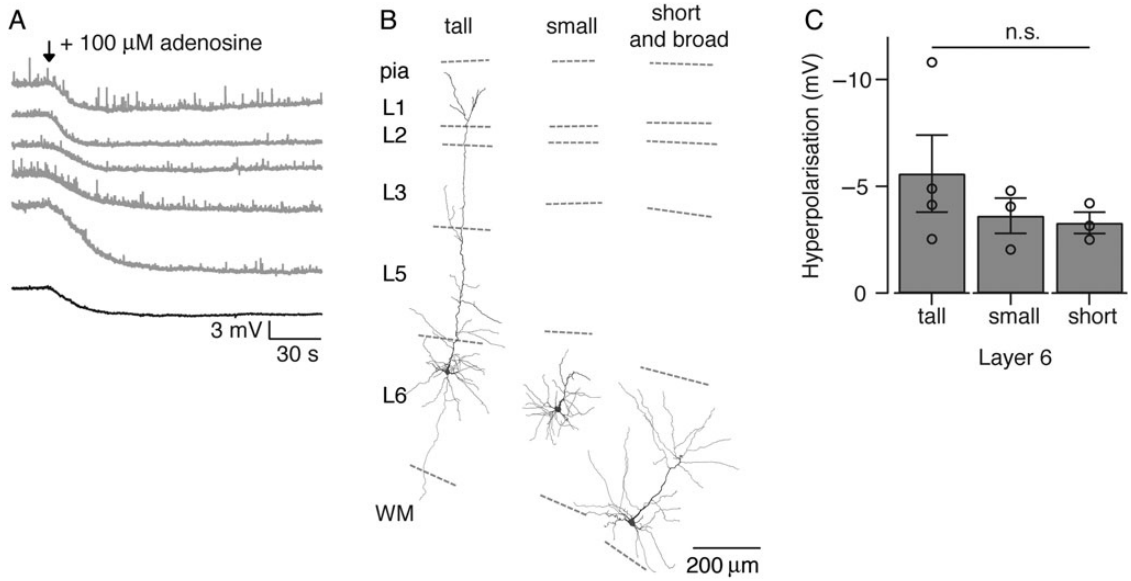

Figure 5. Layer 6 pyramidal neurons are sensitive for adenosine. (*A*) Example traces of the RMP during bath application of 100 µM adenosine (start at arrow). Average response is shown in black (bottom, $n = 13$). (*B*) Morphological reconstruction of soma and dendrites from L6 pyramidal cells with apical dendrites reaching layer 1 ("tall"), or staying in layer 5–6 ("small" and "short and broad"). Small L6 neurons possessed more confined dendrites compared with "short and broad" L6 neurons. Note, however, the large morphological variability of L6 neurons. (*C*) Adenosine-induced hyperpolarization of the RMP for the different L6 morphological subtypes (tall, $n = 4$; small, $n = 3$, short and broad, $n = 3$; $P = 0.46$).

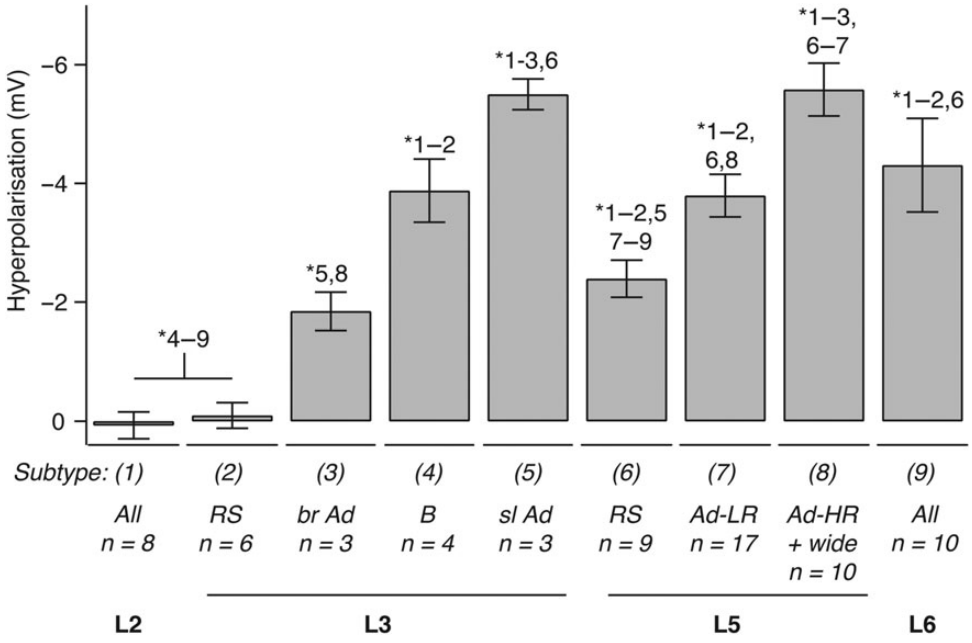

Figure 6. Summary. Average adenosine-induced hyperpolarization for pyramidal neurons in layers (L)2–6. Results from pair-wise comparisons in post hoc tests are shown using the subtype number as indicated within brackets at the *x*-axis. For example, L6 pyramidal neurons differed significantly with L2, RS L3, and RS L5 pyramidal neurons (subtypes 1, 2, and 6, respectively). $^*P < 0.05$.

Heterogeneity of Adenosine Sensitivity Is Also Apparent in Rat Somatosensory Cortex

Our findings suggest that adenosine differentially affects pyramidal cells in a neuronal subtype and layer-specific way. To test if this applies also to other cortical regions, we examined the effects of adenosine application on pyramidal neurons in the rat somatosensory cortex. For this, we studied the effect of adenosine on L2 and different types of L5 pyramidal neurons in the somatosensory cortex.

First, we examined pyramidal neurons from the upper part of layer 2/3 of the somatosensory cortex. The membrane potential of pyramidal neurons in upper layer 2 did not hyperpolarize in response to adenosine application (Fig. 7*A*,*B* and Table 2). Other passive membrane properties remained also

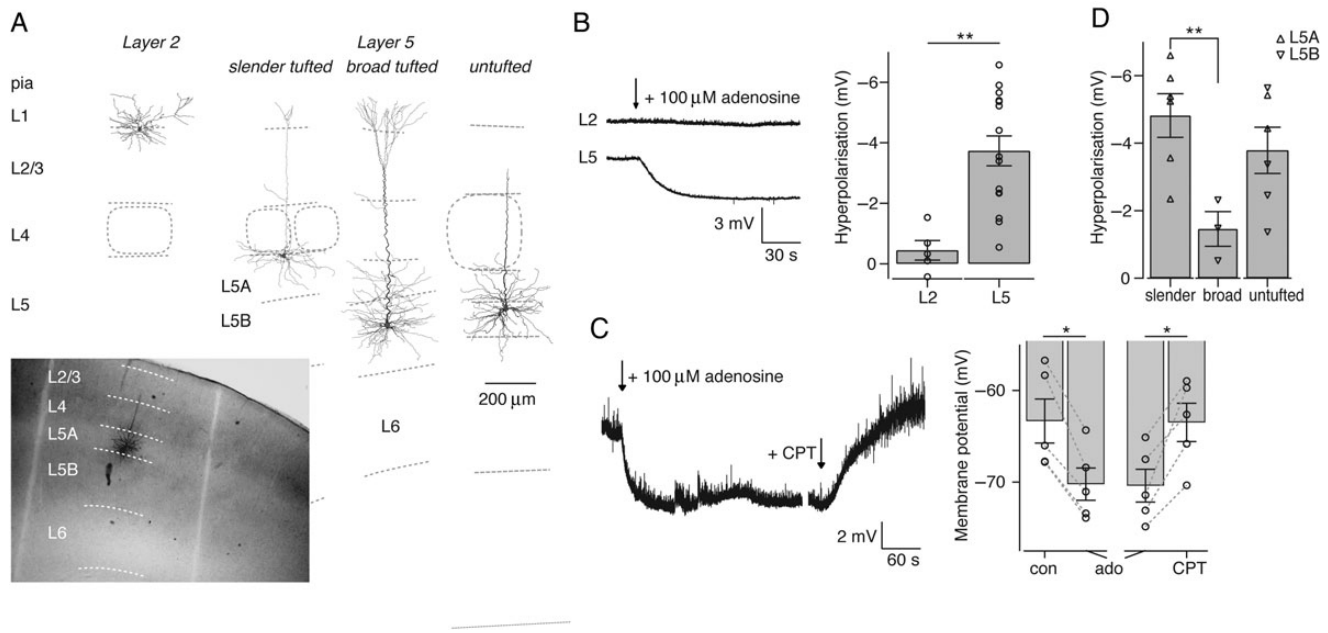

Figure 7. Heterogeneity of adenosine sensitivity is also apparent in rat somatosensory cortex. Heterogeneity of adenosine sensitivity is also apparent in rat somatosensory cortex. (*A*) Morphological reconstruction of the soma and dendrites from pyramidal neurons in layers 2 and 5 of the somatosensory cortex. Inset at left bottom shows an example staining with layer borders indicated as dotted lines. (*B*) Left, average response of the RMP of excitatory neurons in layers 2 and 5 during bath application of 100 µM adenosine (start at arrow). Right, average adenosine-induced hyperpolarization of layer 2 pyramidal neurons ($n = 5$) and layer 5 pyramidal neurons ($n = 15$). (*C*) Example trace of the RMP during application of 100 µM adenosine, followed by coapplication of 5 µM A1R antagonist CPT. Right, average responses during control (con) and 100 µM adenosine (ado) conditions, and during coapplication of 1–5 µM CPT ($n = 5$). (*D*) Adenosine-induced hyperpolarization of the RMP for layer 5 pyramidal neuron subtypes (slender tufted, $n = 6$; broad tufted, $n = 3$; untufted, $n = 6$). Sublaminar location of neurons is indicated for layer 5A (upward triangles) or 5B (downward filled triangles). $^*P < 0.05$, $^{**}P < 0.01$.

Table 2

Adenosine modulation of passive properties of pyramidal neurons in rat somatosensory cortex

	Control	100 µM adenosine	Wash	*P*
Layer 2 pyramidal neurons ($n = 5$)				
RMP (mV)	−81.3 ± 1.7	−81.7 ± 1.7	–	0.25
Input resistance (MΩ)	184 ± 29	184 ± 27	190 ± 30 ($n = 4$)	0.96
Time constant (ms)	21.0 ± 2.7	22.2 ± 1.9	26.1 ± 1.6 ($n = 4$)	0.62
Rheobase (pA)	208 ± 30	226 ± 49	218 ± 40 ($n = 4$)	0.44
Layer 5 pyramidal neurons ($n = 14$)				
RMP (mV)	−65.8 ± 1.0 ($n = 15$)	−69.5 ± 1.1 ($n = 15$)	–	<0.01
Input resistance (MΩ)	130 ± 16	116 ± 14	149 ± 2 ($n = 12$)	0.04/<0.01
Time constant (ms)	20.3 ± 1.1	17.6 ± 1.1	24.6 ± 1.7 ($n = 12$)	0.04/<0.01
Rheobase (pA)	169 ± 32	229 ± 36	148 ± 33 ($n = 12$)	<0.01/<0.01

Note: Average ± SEM; RMP, resting membrane potential. *P* lists the results from paired *t*-tests between control and adenosine. When $P < 0.10$ the result from the paired *t*-test between adenosine and wash-out is also given.

unchanged (Table 2) in agreement with our results in L2 pyramidal neurons of the prefrontal cortex.

In contrast, L5 pyramidal neurons of the somatosensory cortex responded to bath application of 100 µM adenosine with a hyperpolarization of the RMP (Fig. 7*A*,*B* and Table 2). The membrane potential could be reversed to control values by application of 2–5 µM of the adenosine A_1 receptor antagonist CPT [Fig. 7*C*, RMP −63.3 ± 2.4 mV (control), −70.4 ± 1.8 mV (adenosine), −63.5 ± 2.1 mV (CPT), $n = 5$, paired *t*-test $P < 0.01$]. In addition, adenosine application changed passive cell properties and reduced cell excitability of L5 pyramidal neurons (Table 2).

L5 pyramidal neurons in the rat somatosensory cortex are commonly categorized in 3 cell classes: (1) Slender tufted pyramidal neurons that possess only a simple apical dendritic tree, (2) broad tufted pyramidal neurons with elaborate apical dendrites, and (3) pyramidal neurons with virtually untufted and often short apical dendrites (Larsen and Callaway 2006; De Kock et al. 2007; Hattox and Nelson 2007; Le Be et al. 2007; Feldmeyer 2012; Oberlaender et al. 2012). Slender tufted pyramidal neurons are typically found in the upper part of layer 5, sublamina 5A, whereas thick-tufted and untufted pyramidal neurons are mostly found in lower sublamina 5B (Chmielowska et al. 1989; Manns et al. 2004; Feldmeyer et al. 2005; Larsen et al. 2007; Feldmeyer 2012).

We found that slender tufted L5 pyramidal neurons showed a greater membrane hyperpolarization after adenosine application than broad tufted L5 pyramidal neurons [Fig. 7*D* and Table 3, adenosine-induced hyperpolarization −4.8 ± 0.6 (slender, $n = 6$), −1.5 ± 0.5 (broad, $n = 3$), −3.8 ± 0.7 (untufted, $n = 6$), ANOVA $P < 0.01$, post hoc Tukey test $P < 0.05$]. Untufted pyramidal neurons displayed more variable responses (Fig. 7*D*). When we

categorized pyramidal neurons according to their sublaminar location, L5A neurons were on average more sensitive to adenosine application than L5B neurons [Fig. 7*D*, −4.8 ± 0.5 (L5A, $n = 8$), −2.5 ± 0.6 (L5B, $n = 7$), $P < 0.01$].

Thus, in somatosensory cortex as in the mPFC, adenosine affects pyramidal neurons in a cell type-dependent manner.

Fast-Spiking and Low-Threshold Spiking Interneurons Are Insensitive to Adenosine

Although most studies described in the literature have focused on the effect of adenosine on excitatory neurotransmission, some papers suggest that the synaptic input to or from interneurons is also modified by adenosine (Yoon and Rothman 1991; Fontanez and Porter 2006; Kruglikov and Rudy 2008). However, the direct effect of adenosine on cortical interneurons has not been examined. We therefore made whole-cell patch-clamp recordings from interneurons and bath-applied 100 μM adenosine.

Table 3
Properties of L5 pyramidal subtypes in the somatosensory cortex

	Broad tufted ($n = 3$)	Slender tufted ($n = 6$)	Untufted ($n = 6$)	*P*
Width apical tuft (μm)	**376 ± 46***	**129 ± 21**/***	**26 ± 18****	**<0.01**
Width basal dendrites (μm)	427 ± 42	356 ± 15	335 ± 26	0.11
RMP (mV)	−64.3 ± 1.3	−67.8 ± 1.2	−69.1 ± 1.3	0.10
Ratio ISI-1/ISI-9	0.46 ± 0.20	0.22 ± 0.05	0.05 ± 0.01	**0.01**
Ratio ISI-2/ISI-9	1.00 ± 0.09	0.64 ± 0.08	0.56 ± 0.13	0.07
Ratio ISI-3/ISI-9	0.99 ± 0.02	0.84 ± 0.03	0.88 ± 0.09	0.42
Input resistance (MΩ)	**55 ± 11***	146 ± 10	146 ± 28	**0.04**
Time constant (ms)	16.3 ± 1.1	22.1 ± 1.1	18.6 ± 2.0	0.10
Rheobase (pA)	**370 ± 68***	120 ± 8	130 ± 19	**<0.01**
Voltage sag (mV, 100 pA)	28.7 ± 4.7	19.3 ± 3.0	21.5 ± 5.1	0.43
Adenosine effect (mV)	−1.5 ± 05	−4.8 ± 0.6	−3.8 ± 0.7	**0.03**

Note: Average ± SEM; RMP, resting membrane potential. *P* lists the results from the ANOVA test. For clarity, the results of the post hoc comparison of groups is only given (values in bold followed with asterisks) when a cell type is different from all other cell types.
*$P < 0.01$.
**$P < 0.05$.

In the rodent (prefrontal) cortex, interneurons have been categorized into several different subtypes based on their electrophysiological, morphological, and chemical properties (Kawaguchi and Kondo 2002; Beierlein et al. 2003; Couey et al. 2007; Ascoli et al. 2008; Fanselow et al. 2008; Van Aerde et al. 2009). Here, we distinguished 2 main interneuron classes on the basis of their AP firing pattern and passive properties: (1) Fast-spiking (FS) interneurons that were characterized by their sustained high-frequency firing upon current injection, and (2) low-threshold spiking (LTS) interneurons that possessed low rheobase values (Fig. 8*A*,*B* and Table 4). FS and LTS interneurons differed not only in firing rate and cell excitability, but also in other physiological properties (Table 4).

In contrast to pyramidal cells, the interneurons examined in our study did not hyperpolarize in response to adenosine application. This was the case for both interneurons types, in all layers of the cortex. Because we found no difference between interneurons from different layers, we grouped interneurons per interneuron type only (Fig. 8*C* and Table 5). In agreement with these results, passive membrane properties also remained unchanged after adenosine application (Table 5).

Next, we examined interneurons in the somatosensory cortex. For the somatosensory cortex we used a rough distinction based on the firing pattern, that is, we differentiated only between "FS" and "adapting, non-FS" interneurons (Table 4). In contrast to FS interneurons, non-FS interneurons showed marked adaptation of AP firing upon current injection (Table 4). Both FS and non-FS interneurons did not hyperpolarize in response to adenosine application (Fig. 8*C*).

Thus, adenosine does not seem to modulate cell excitability in the interneuron types studied here.

Size of Adenosine Response Is Correlated with Passive Cell Properties and Cell Morphology

Because of the profound differences in passive membrane properties between pyramidal neurons in different cortical layers and between specific neuronal subtypes within cortical layers, we wondered if there was a correlation between passive

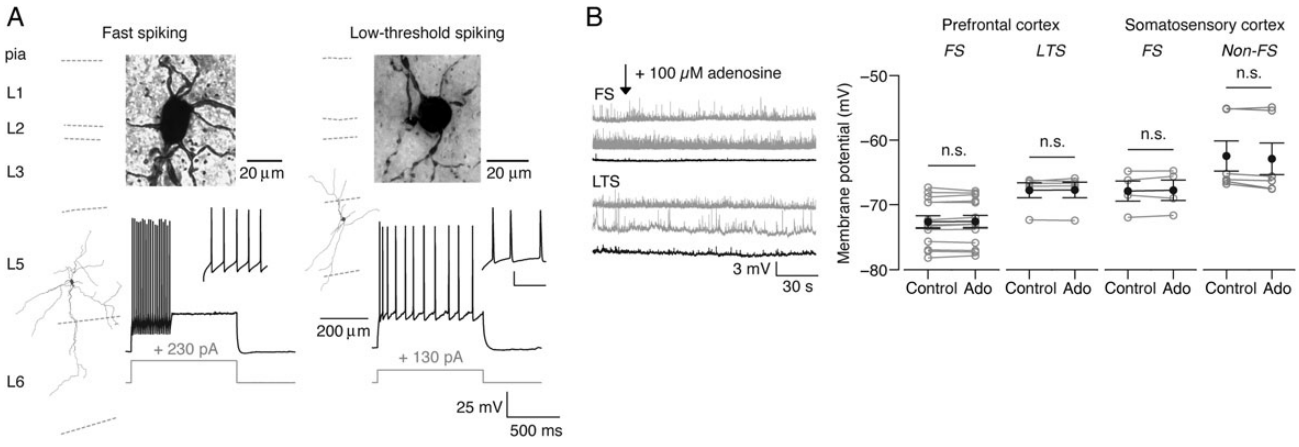

Figure 8. Interneurons are insensitive to adenosine. (*A*) Top, morphological reconstruction of the dendrites of interneurons with FS (left) or LTS (right) characteristics. Cortical layers are indicated. Note the nonpyramidal shape of the cell bodies. Bottom, corresponding electrophysiological profile shows the response when minimally 10 APs were elicited with corresponding current steps in gray. The inset shows a magnification of the first spikes (scale bar: 25 mV, 50 ms). (*B*) Example traces of the RMP of FS interneurons (top) and LTS interneurons (bottom) in medial prefrontal cortex (mPFC) during bath application of 100 μM adenosine (start at arrow). Average responses are shown in black (FS, $n = 18$; LTS, $n = 5$). Right, average RMP during control and adenosine (ado) conditions for FS interneurons and LTS interneurons in the prefrontal cortex, and FS and non-FS interneurons in the somatosensory cortex. Note that some non-FS interneurons were recorded with depolarizing current injections to increase the driving force for potassium. The change in membrane potential was not significant (FS in mPFC, $n = 14$, $P = 0.43$; LTS in mPFC, $n = 5$, $P = 0.71$; FS in somatosensory cortex, $n = 4$, $P = 0.65$; non-FS in somatosensory cortex, $n = 6$, $P = 0.27$).

Table 4
Properties of interneuron subtypes in prefrontal and somatosensory cortex

	mPFC			Somatosensory		
	LTS ($n = 5$)	FS ($n = 14$)	P	Non-FS ($n = 6$)	FS ($n = 4$)	P
Spike half-width (ms)	0.79 ± 0.05	0.38 ± 0.03	<0.01	0.37 ± 0.04	0.20 ± 0.02	0.01*
Ratio ISI-1/ISI-9	0.43 ± 0.09	0.96 ± 0.04	<0.01	0.15 ± 0.02	0.70 ± 0.07	<0.01**
Ratio ISI-2/ISI-9	0.53 ± 0.10	0.95 ± 0.03	<0.01	0.24 ± 0.06	0.80 ± 0.05	<0.01**
Ratio ISI-3/ISI-9	0.59 ± 0.10	1.02 ± 0.06	<0.01	0.36 ± 0.07	1.08 ± 0.26	0.01*
Slope F-I (Hz/100 pA)	13.6 ± 2.0	40.9 ± 4.4	<0.01	11.6 ± 2.6	46.6 ± 5.1	<0.01**
RMP (mV)	−66.3 ± 1.9	−72.2 ± 1.3	<0.01	−65.0 ± 0.4	−68.0 ± 1.3	0.07
Input resistance (MΩ)	361 ± 58	178 ± 11	<0.01	83 ± 13	135 ± 26	0.68
Time constant (ms)	27.4 ± 5.2	7.9 ± 0.5	<0.01	7.4 ± 0.6	8.0 ± 0.8	0.56
Rheobase (pA)	28 ± 9	176 ± 15	<0.01	234 ± 52	163 ± 43	0.66

Note: Average ± SEM; RMP, resting membrane potential.
*$P < 0.05$.
**$P < 0.01$.

Table 5
Adenosine does not modulate passive properties of mPFC interneurons

	Control	100 μM Adenosine	Wash	P
FS interneurons in mPFC ($n = 14$)				
RMP (mV)	−72.7 ± 0.9	−72.6 ± 0.9	72.3 ± 1.0	0.43
Input resistance (MΩ)	171 ± 12	175 ± 11	182 ± 14	0.57
Time constant (ms)	8.6 ± 0.8	9.1 ± 0.7	10.0 ± 0.5	0.52
Rheobase (pA)	184 ± 17	196 ± 17	179 ± 17	0.41
LTS interneurons in mPFC ($n = 5$)				
RMP (mV)	−67.8 ± 1.2	−67.7 ± 1.2	–	0.71
Input resistance (MΩ)	391 ± 64	438 ± 70	369 ± 43	0.17
Time constant (ms)	30.2 ± 5.6	41.0 ± 6.6	31.2 ± 9.3	0.17
Rheobase (pA)	20 ± 6	43 ± 10	53 ± 14	0.06/0.25

Note: Average ± SEM; RMP, resting membrane potential. P lists the results from paired t-tests between control and adenosine. When $P < 0.10$ the result from the paired t-test between adenosine and wash-out is also given.

membrane properties and the size of the adenosine-induced hyperpolarization in our complete data set from the prefrontal cortex ($n = 68$). Indeed, significant correlations were found for cellular input resistance, membrane time constant, RMP, and rheobase current (Fig. 9).

In contrast, although correlations of spike-time adaptation (i.e., RS or adapting/bursting profiles) and adenosine sensitivity were observed for pyramidal neurons within layer 3 or 5 as described above, these correlations were not observed when the complete data set was analyzed (Fig. 9*E*). This implies that passive properties are a better predictor of adenosine sensitivity than spike-time adaptation per se.

Pyramidal cell morphology was also moderately correlated with the adenosine sensitivity: Pyramidal neurons with slender apical dendritic tufts showed on average a larger response to adenosine than pyramidal neurons with broad apical tufts (Fig. 9*F*).

Discussion

The present study demonstrates that the neuromodulator adenosine, which plays an important role in sleep homeostasis, does not exercise a general inhibitory tone on the cortical network as previously hypothesized, but rather specifically modulates each pyramidal neuron subtype in a distinct fashion (Fig. 10). Our results from interneurons and pyramidal neurons in the rat mPFC are likely to apply to neurons in other cortical areas, as we obtained similar results for the rat somatosensory cortex. Adenosine decreased cellular excitability of most pyramidal neuron subtypes via adenosine A_1 receptors that lead to the opening of potassium channels. Furthermore, passive properties like cellular input resistance, membrane time constant, RMP, and cellular excitability were correlated with the size of the adenosine response, as well as the relative field span of the apical dendritic tuft.

Heterogeneity of Adenosine Is Distinct from Modulation by Other Neuromodulators

Neuromodulators such as acetylcholine, noradrenaline, dopamine, and serotonin have different effects on different pyramidal cell subtypes, or on pyramidal neurons in different layers. Laminar heterogeneity of excitatory neurons has been described for the transient and sustained effects of acetylcholine on rat somatosensory and prefrontal cortex (Gulledge and Stuart 2005; Gulledge et al. 2007; Eggermann and Feldmeyer 2009) and for nicotinic modulation of pyramidal neurons and interneurons in the mPFC (Poorthuis et al. 2013). Interestingly, some of these studies found unresponsive pyramidal neurons in the superficial layers of the mPFC (Gulledge et al. 2007; Poorthuis et al. 2013). Although no detailed electrophysiological and morphological analyses were performed to distinguish between L2 and (subtypes of) L3 pyramidal neurons, these results seem to be reminiscent of the insensitivity to adenosine we found for L2 and RS L3 pyramidal neurons.

In a number of studies, the neuromodulatory effects on different types of L5 pyramidal neurons in the mPFC have been examined. Although different methods have been used to distinguish between L5 pyramidal neuron subtypes, the correlation between electrophysiology, morphology, and projection targets allows a comparison between the various studies. In general, broad tufted pyramidal neurons are characterized by RS firing patterns, low R_{in}, and large voltage sags and axonal projections to the thalamus or the brainstem. Slender tufted L5 pyramidal neurons have adaptive firing patterns, a high R_{in}, and a lower voltage sag, and their axon targets the contralateral cortex and striatum (Wang et al. 2006; Otsuka and Kawaguchi 2008; Dembrow et al. 2010; Avesar and Gulledge 2012). The most striking effect has been found for serotonin, which hyperpolarizes the majority of L5 pyramidal neurons via the serotonin 5-HT_{1A} receptor, but depolarizes a small subpopulation of L5 pyramidal neurons that exclusively express the 5-HT_{2A} receptor (Beique et al. 2007). The latter pyramidal

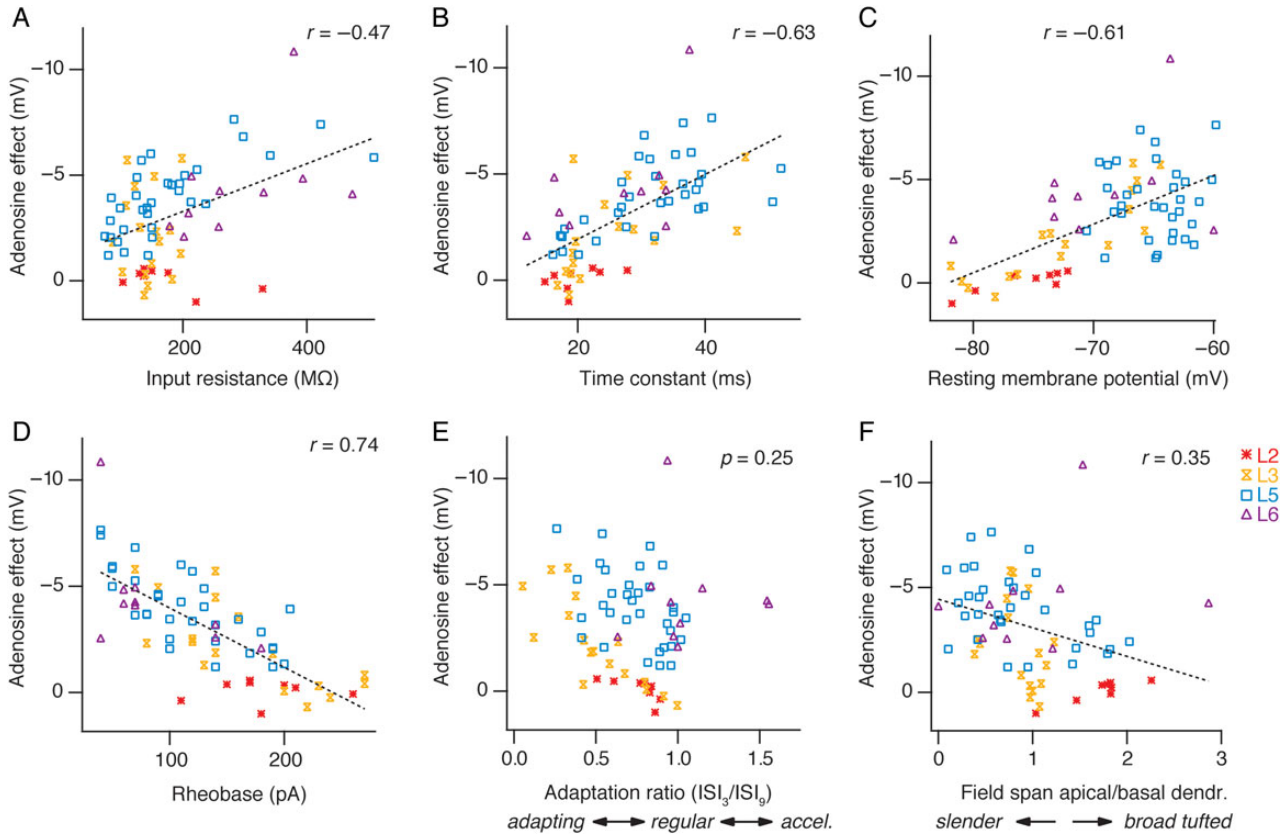

Figure 9. Correlation between cellular properties and adenosine sensitivity. (*A–F*) Size of adenosine-induced hyperpolarization as a function of cellular input resistance (*A*), membrane time constant (*B*), RMP (*C*), rheobase current (*D*), spike-time adaptation (*E*, ISI 3 divided by ISI-9. Accel., accelerating), and cell morphology (*F*, the ratio of the spanning width of apical/basal dendrites is taken as a measure for the slenderness or broadness of apical tufts). Linear fits are shown as black dashed line. Pyramidal neurons from layer 2 (red asterisks), layer 3 (yellow hourglass), layer 5 (blue squares), and layer 6 (purple triangles) were grouped for correlation analysis ($n = 68$, $P < 0.01$, unless otherwise indicated).

neurons were subsequently identified as callosal/commisural L5 neurons that project onto the contralateral cortex (Avesar and Gulledge 2012). Dopamine D1 receptor expression was found in a subpopulation of slender tufted adapting L5 neurons, whereas dopamine D2 receptor activation was found to be specific for thick-tufted L5 pyramidal neurons (Gee et al. 2012; Seong and Carter 2012). Broad tufted RS L5 pyramidal neurons were more sensitive to adrenaline and acetylcholine than slender tufted adapting neurons in the same layer (Dembrow et al. 2010). In contrast, slender tufted adapting L5 pyramidal neurons are more sensitive to adenosine (i.e., showed on average a larger hyperpolarization) than broad tufted RS L5 neurons that were primarily modulated by adrenergic, muscarinic, and D2 agonists (see Supplementary Table for an overview of discussed studies). Moreover, we found a differential adenosine sensitivity for 2 slender tufted adapting subtypes, namely those with a high R_{in} and sparse basal dendrites, and those with lower R_{in} and more numerous basal dendrites. This may suggest that these slender tufted L5 pyramidal cell subtypes fulfill different roles in signal processing in the mPFC. Whether these slender tufted subtypes have different projection targets is unknown.

As described above, a substantial body of the literature exists on the differential responsiveness of L5 pyramidal neuron subtypes to neuromodulators. However, to our knowledge, such studies have not been performed for L3 pyramidal neurons, and our study is the first to report a differential neuromodulation of specific subtypes of pyramidal neurons in superficial cortical layers.

In contrast to the very heterogeneous adenosine responsiveness of mPFC pyramidal neuron subtypes, the 2 classes of cortical interneurons we investigated were very uniform in their insensitivity to adenosine. This result fits well in the scheme that adenosine decreases cortical activity and shifts the balance to inhibition over excitation, although our work is the first to examine the "direct" effect of adenosine on cortical interneurons. However, because adenosine receptors may also be present at presynaptic sites, adenosine may inhibit excitatory synaptic input to interneurons. Future experiments that record the excitatory and inhibitory synaptic inputs to cortical interneurons are required to investigate the presynaptic effects of adenosine for interneurons on the neocortex.

Functional Implications

The differential sensitivity of pyramidal neurons, and the insensitivity of cortical interneurons to the neuromodulator adenosine found in both rat medial prefrontal and somatosensory cortex, could have important implications for cortical information processing under conditions of high adenosine levels, such as during prolonged wakefulness, during the first hours of recovery sleep, and after chronic exposure to opiates (Porkka-Heiskanen et al. 2000; Dunwiddie and Masino 2001; Lu et al. 2010). It is at present unclear to what level the

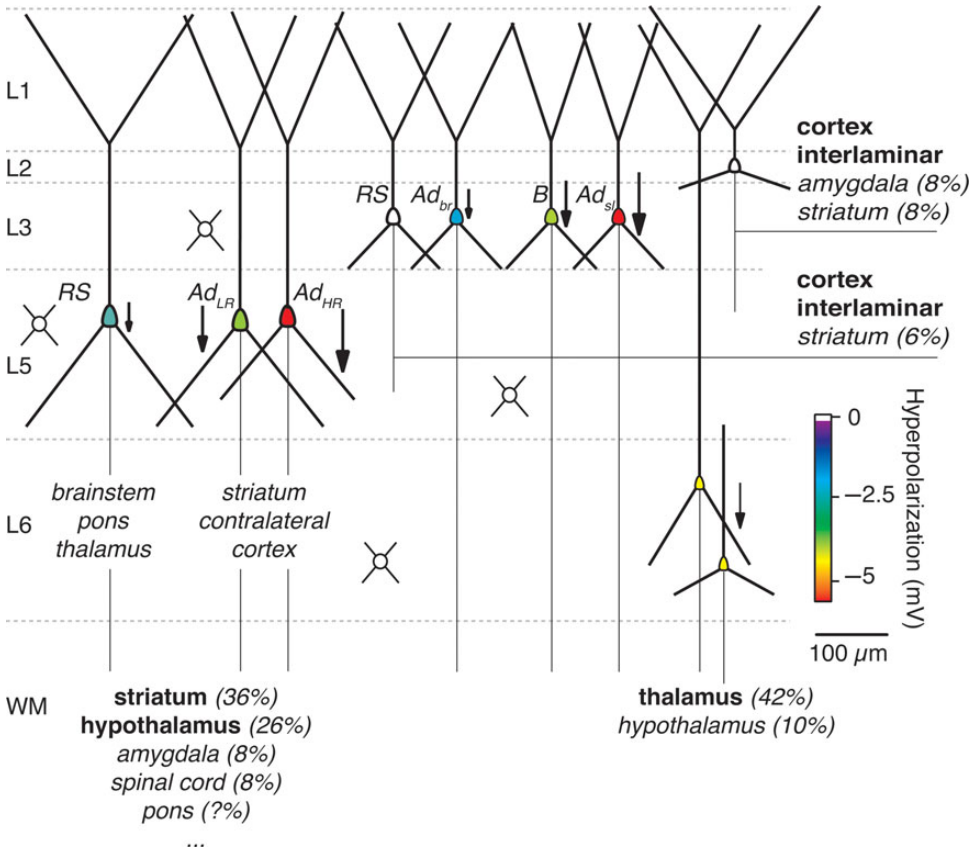

Figure 10. Adenosine decreases cell excitability of pyramidal neurons in a layer- and subtype-specific way, while leaving interneuron excitability unaffected. Schematic summary of the effects of adenosine on pyramidal and interneurons in layer (L) 2–6 of the prefrontal cortex microcircuit. Arrows and color indicate the size of the adenosine-induced decrease in cell excitability of L2–6 pyramidal neurons (filled neurons). Interneurons (round somata) and pyramidal neurons with white somas are not affected by adenosine. Percentages for main subcortical projection areas are from Gabbott et al. (2005), and projection areas for RS and Ad subtypes in layer 5 are adapted from Dembrow et al. (2010) and Gee et al. (2012). Dendrites are depicted with thick lines, axons with thin lines. WM, white matter.

extracellular concentration of adenosine can rise under physiological or pathophysiological conditions. However, recent studies that made use of adenosine biosensors show that the adenosine concentration is nonuniform, suggesting the presence of hotspots or microdomains where the adenosine concentration is higher compared with the rest of the extracellular space (Wall et al. 2007; Klyuch et al. 2012; Schmitt et al. 2012). Thus, results from microdialysis studies that show increases in adenosine concentrations under certain situations probably reflect much larger local increases in adenosine concentrations. Future studies are needed to investigate possible (subcellular) locations of such hotspots or microdomains.

Layer 2 of the mPFC receives synaptic inputs from other association cortices, the hippocampus, amygdala, and midline thalamus, and it relays these inputs to deeper layers as well as projecting onto other cortical areas and onto the basolateral amygdala and ventral striatum (Cauller 1995; Douglas and Martin 2004; Gabbott et al. 2005; Little and Carter 2012). Adenosine did not affect cellular excitability of layer 2 neurons, and hence the initial processing of these inputs would not be expected to be impaired (Fig. 10). Potentially, the insensitivity of these neurons to adenosine could explain why some learning tasks, such as cued fear conditioning, are not affected by sleep deprivation (Graves et al. 2003). Cued fear conditioning is hippocampus independent and relies on amygdala function, one of the areas to which L2 pyramidal neurons project (Gabbott et al. 2005).

In contrast, synaptic inputs onto L5 or L6 pyramidal neurons originating from the thalamus or from inter- and intralaminar connection arrive on pyramidal neurons that are less excitable under conditions of high adenosine levels; thus, subcortical–cortical and intralaminar processing are reduced in these conditions. As L5 and L6 pyramidal neurons primarily project onto subcortical areas, this could result in a shift from cortico-subcortical processing to corticocortical processing (Fig. 10). However, adenosine can also assert its inhibiting effect via adenosine receptors at presynaptic terminals and reduce the probability of synaptic vesicle release (Fontanez and Porter 2006; Kerr et al. 2013). In this way, adenosine could severely affect synaptic transmission and reduce synaptic input to pyramidal neurons. So far, it is not known if adenosine receptors are differentially expressed on synaptic terminals of pyramidal neurons in different layers. Future experiments investigating the synaptic transmission between, for example, L2 pyramidal neurons and several defined inputs are needed to determine if and which synaptic inputs to L2 and RS L3 pyramidal neurons are modulated by adenosine.

The decreased output to the various subcortical projection areas of mPFC L5 and L6 pyramidal neurons could explain some of the behavioral changes that are associated with increased levels of adenosine. Local infusion of adenosine in rat prefrontal cortex affects wakefulness and acetylcholine release in both prefrontal cortex and the pontine reticular formation (Van Dort et al. 2009). We suggest that this effect may be

mediated by broad tufted RS L5 pyramidal neurons forming connections with the pontine nuclei. Although the mechanisms by which these neurons regulate the function of the pontine nuclei require further studies, a possible pathway could be a direct connection between prefrontal L5 pyramidal neurons and the cholinergic neurons in the pontine nuclei: When adenosine decreases L5 pyramidal neuron input to these cholinergic neurons, this could lead to a decreased acetylcholine concentration in the pontine nuclei and thus, a reduced activation of the wake promoting reticular activating system. Other L5 projection areas are the striatum and hypothalamus that modulate the motivational state (Gabbott et al. 2005). Adenosine modulation of projection neurons to these areas could explain the decrease in motivation that human subjects experience after prolonged wakefulness. The reduced excitability of L6 pyramidal neurons could affect arousal and awareness via their projection to the mediodorsal thalamus (Van Der Werf et al. 2002; Gabbott et al. 2005). Moreover, although no direct connections from the mPFC to the hippocampus have been identified, L6 pyramidal neurons are responsible for the main indirect connection to the hippocampus via the nucleus reuniens in the medial thalamus (Vertes et al. 2007). The decreased excitability of L6 pyramidal neurons could therefore contribute to the deficits in hippocampus-dependent learning that occur after sleep deprivation (Graves et al. 2003; Van Der Werf et al. 2009). In addition, the reduced excitability of individual L5 and L6 pyramidal neurons will most likely result in a decreased ability of the mPFC to sustain recurrent excitation, one of the mechanisms thought to underlie working memory (Goldman-Rakic 1995; Wang 1999). Indeed, working memory and attention tasks are impaired during prolonged wakefulness and can be improved by adenosine antagonists, such as caffeine, present in coffee and tea (Fredholm et al. 1999; Harrison et al. 2000).

The effects of adenosine are not only restricted to the medial prefrontal cortex, but also apply to the somatosensory cortex. Thus, under conditions of high adenosine levels, sensory processing will most likely be affected owing to the reduced excitability of L5 pyramidal neurons in the somatosensory cortex. Several studies report changes in cortical activity in response to visual or auditory stimuli after subjects have undergone sleep deprivation (Oken et al. 2006; Chee et al. 2008; Bortoletto et al. 2011). However, whether these impairments result from changes in motivational or attentional processes or from local effects of adenosine remains to be further elucidated.

In summary, the present study demonstrates that the neuromodulator adenosine, which plays an important role in sleep homeostasis, does not exercise a uniform and general inhibitory tone on the cortical network as previously assumed, but rather decreases cell excitability of pyramidal neurons in a layer- and subtype-specific way, while leaving interneuron excitability unaffected. Both passive electrical properties, reflecting ion channels expression, and dendritic morphology were correlated with the amplitude of the adenosine response. The decreased excitability of subcortically projecting L5 and L6 neurons may contribute to the reduced output or executive functions of the prefrontal cortex during prolonged wakefulness and sleep deprivation, potentially explaining some of the effects of sleep deprivation on cognitive function (Graves et al. 2003; Walker 2008; Halassa et al. 2009; Van Der Werf et al. 2009; Killgore 2010).

Supplementary Material

Supplementary material can be found at: http://www.cercor.oxfordjournals.org/.

Funding

This work was supported by the Deutsche Forschungsgemeinschaft (DFG-SNF Research group 'BaCoFun') and the Helmholtz Alliance for Systems Biology. Funding to pay the Open Access publication charges for this article was provided by the Institute of Neuroscience and Medicine 2 (INM-2) of the Research Center Jülich.

Notes

We thank Werner Hucko for excellent technical assistance and Andreas Kriebel and Liang Dongling for help with morphological reconstructions. We thank Ted Abel (University of Pennsylvania) for his helpful discussion and useful comments on this manuscript. *Conflict of Interest*: None declared.

References

Agmon A, Connors BW. 1992. Correlation between intrinsic firing patterns and thalamocortical synaptic responses of neurons in mouse barrel cortex. J Neurosci. 12:319–329.

Arrigoni E, Chamberlin NL, Saper CB, Mccarley RW. 2006. Adenosine inhibits basal forebrain cholinergic and noncholinergic neurons in vitro. Neuroscience. 140:403–413.

Ascoli GA, Alonso-Nanclares L, Anderson SA, Barrionuevo G, Benavides-Piccione R, Burkhalter A, Buzsaki G, Cauli B, Defelipe J, Fairen A et al. 2008. Petilla terminology: nomenclature of features of GABAergic interneurons of the cerebral cortex. Nat Rev Neurosci. 9:557–568.

Avesar D, Gulledge AT. 2012. Selective serotonergic excitation of callosal projection neurons. Front Neural Circuits. 6:12.

Bailey CD, Alves NC, Nashmi R, De Biasi M, Lambe EK. 2012. Nicotinic alpha5 subunits drive developmental changes in the activation and morphology of prefrontal cortex layer VI neurons. Biol Psychiatry. 71:120–128.

Basheer R, Strecker RE, Thakkar MM, McCarley RW. 2004. Adenosine and sleepwake regulation. Prog Neurobiol. 73:379–396.

Beierlein M, Gibson JR, Connors BW. 2003. Two dynamically distinct inhibitory networks in layer 4 of the neocortex. J Neurophysiol. 90:2987–3000.

Beique JC, Imad M, Mladenovic L, Gingrich JA, Andrade R. 2007. Mechanism of the 5-hydroxytryptamine 2a receptor-mediated facilitation of synaptic activity in prefrontal cortex. Proc Natl Acad Sci USA. 104:9870–9875.

Boison D. 2011. Methylxanthines, seizures, and excitotoxicity. Handb Exp Pharmacol. 200:251–266.

Bortoletto M, Tona Gde M, Scozzari S, Sarasso S, Stegagno L. 2011. Effects of sleep deprivation on auditory change detection: a n1-mismatch negativity study. Int J Psychophysiol. 81:312–316.

Cauller L. 1995. Layer I of primary sensory neocortex: where top-down converges upon bottom-up. Behav Brain Res. 71:163–170.

Chang YM, Luebke JI. 2007. Electrophysiological diversity of layer 5 pyramidal cells in the prefrontal cortex of the rhesus monkey: in vitro slice studies. J Neurophysiol. 98:2622–2632.

Chee MW, Tan JC, Zheng H, Parimal S, Weissman DH, Zagorodnov V, Dinges DF. 2008. Lapsing during sleep deprivation is associated with distributed changes in brain activation. J Neurosci. 28:5519–5528.

Chmielowska J, Carvell GE, Simons DJ. 1989. Spatial organization of thalamocortical and corticothalamic projection systems in the rat SMI barrel cortex. J Comp Neurol. 285:325–338.

Couey JJ, Meredith RM, Spijker S, Poorthuis RB, Smit AB, Brussaard AB, Mansvelder HD. 2007. Distributed network actions by nicotine increase the threshold for spike-timing-dependent plasticity in prefrontal cortex. Neuron. 54:73–87.

Cunha RA. 2001. Adenosine as a neuromodulator and as a homeostatic regulator in the nervous system: different roles, different sources and different receptors. Neurochem Int. 38:107–125.

Degenetais E, Thierry AM, Glowinski J, Gioanni Y. 2002. Electrophysiological properties of pyramidal neurons in the rat prefrontal cortex: an *in vivo* intracellular recording study. Cereb Cortex. 12:1–16.

De Kock CP, Bruno RM, Spors H, Sakmann B. 2007. Layer- and cell-type-specific suprathreshold stimulus representation in rat primary somatosensory cortex. J Physiol. 581:139–154.

Dembrow NC, Chitwood RA, Johnston D. 2010. Projection-specific neuromodulation of medial prefrontal cortex neurons. J Neurosci. 30:16922–16937.

Diogenes MJ, Neves-Tome R, Fucile S, Martinello K, Scianni M, Theofilas P, Lopatar J, Ribeiro JA, Maggi L, Frenguelli BG et al. 2014. Homeostatic control of synaptic activity by endogenous adenosine is mediated by adenosine kinase. Cereb Cortex. 24:67–80.

Douglas RJ, Martin KA. 2004. Neuronal circuits of the neocortex. Annu Rev Neurosci. 27:419–451.

Dunwiddie TV, Fredholm BB. 1989. Adenosine a1 receptors inhibit adenylate cyclase activity and neurotransmitter release and hyperpolarize pyramidal neurons in rat hippocampus. J Pharmacol Exp Ther. 249:31–37.

Dunwiddie TV, Masino SA. 2001. The role and regulation of adenosine in the central nervous system. Annu Rev Neurosci. 24:31–55.

Eggermann E, Feldmeyer D. 2009. Cholinergic filtering in the recurrent excitatory microcircuit of cortical layer 4. Proc Natl Acad Sci USA. 106:11753–11758.

Elmenhorst D, Basheer R, Mccarley RW, Bauer A. 2009. Sleep deprivation increases a(1) adenosine receptor density in the rat brain. Brain Res. 1258:53–58.

Elmenhorst D, Meyer PT, Winz OH, Matusch A, Ermert J, Coenen HH, Basheer R, Haas HL, Zilles K, Bauer A. 2007. Sleep deprivation increases a1 adenosine receptor binding in the human brain: a positron emission tomography study. J Neurosci. 27:2410–2415.

Fanselow EE, Richardson KA, Connors BW. 2008. Selective, state-dependent activation of somatostatin-expressing inhibitory interneurons in mouse neocortex. J Neurophysiol. 100:2640–2652.

Feldmeyer D. 2012. Excitatory neuronal connectivity in the barrel cortex. Front Neuroanat. 6:24.

Feldmeyer D, Roth A, Sakmann B. 2005. Monosynaptic connections between pairs of spiny stellate cells in layer 4 and pyramidal cells in layer 5a indicate that lemniscal and paralemniscal afferent pathways converge in the infragranular somatosensory cortex. J Neurosci. 25:3423–3431.

Florian C, Vecsey CG, Halassa MM, Haydon PG, Abel T. 2011. Astrocyte-derived adenosine and a1 receptor activity contribute to sleep loss-induced deficits in hippocampal synaptic plasticity and memory in mice. J Neurosci. 31:6956–6962.

Fontanez DE, Porter JT. 2006. Adenosine a1 receptors decrease thalamic excitation of inhibitory and excitatory neurons in the barrel cortex. Neuroscience. 137:1177–1184.

Fredholm BB, Battig K, Holmen J, Nehlig A, Zvartau EE. 1999. Actions of caffeine in the brain with special reference to factors that contribute to its widespread use. Pharmacol Rev. 51: 83–133.

Gabbott PL, Dickie BG, Vaid RR, Headlam AJ, Bacon SJ. 1997. Local-circuit neurones in the medial prefrontal cortex (areas 25, 32 and 24b) in the rat: morphology and quantitative distribution. J Comp Neurol. 377:465–499.

Gabbott PL, Warner TA, Jays PR, Salway P, Busby SJ. 2005. Prefrontal cortex in the rat: projections to subcortical autonomic, motor, and limbic centers. J Comp Neurol. 492:145–177.

Gee S, Ellwood I, Patel T, Luongo F, Deisseroth K, Sohal VS. 2012. Synaptic activity unmasks dopamine d2 receptor modulation of a specific class of layer V pyramidal neurons in prefrontal cortex. J Neurosci. 32:4959–4971.

Gerber U, Greene RW, Haas HL, Stevens DR. 1989. Characterization of inhibition mediated by adenosine in the hippocampus of the rat in vitro. J Physiol. 417:567–578.

Goldman-Rakic PS. 1995. Cellular basis of working memory. Neuron. 14:477–485.

Graves LA, Heller EA, Pack AI, Abel T. 2003. Sleep deprivation selectively impairs memory consolidation for contextual fear conditioning. Learn Mem. 10:168–176.

Greene RW, Haas HL. 1985. Adenosine actions on ca1 pyramidal neurones in rat hippocampal slices. J Physiol. 366:119–127.

Gulledge AT, Park SB, Kawaguchi Y, Stuart GJ. 2007. Heterogeneity of phasic cholinergic signaling in neocortical neurons. J Neurophysiol. 97:2215–2229.

Gulledge AT, Stuart GJ. 2005. Cholinergic inhibition of neocortical pyramidal neurons. J Neurosci. 25:10308–10320.

Haas HL, Greene RW. 1984. Adenosine enhances after hyperpolarization and accommodation in hippocampal pyramidal cells. Pflugers Arch. 402:244–247.

Halassa MM, Florian C, Fellin T, Munoz JR, Lee SY, Abel T, Haydon PG, Frank MG. 2009. Astrocytic modulation of sleep homeostasis and cognitive consequences of sleep loss. Neuron. 61:213–219.

Harrison Y, Horne JA, Rothwell A. 2000. Prefrontal neuropsychological effects of sleep deprivation in young adults—a model for healthy aging? Sleep. 23:1067–1073.

Hattox AM, Nelson SB. 2007. Layer V neurons in mouse cortex projecting to different targets have distinct physiological properties. J Neurophysiol. 98:3330–3340.

Hirai Y, Morishima M, Karube F, Kawaguchi Y. 2012. Specialized cortical subnetworks differentially connect frontal cortex to parahippocampal areas. J Neurosci. 32:1898–1913.

Huber R, Deboer T, Tobler I. 2000. Topography of EEG dynamics after sleep deprivation in mice. J Neurophysiol. 84:1888–1893.

Huston JP, Haas HL, Boix F, Pfister M, Decking U, Schrader J, Schwarting RK. 1996. Extracellular adenosine levels in neostriatum and hippocampus during rest and activity periods of rats. Neuroscience. 73:99–107.

Kalinchuk AV, Mccarley RW, Porkka-Heiskanen T, Basheer R. 2011. The time course of adenosine, nitric oxide (NO) and inducible no synthase changes in the brain with sleep loss and their role in the non-rapid eye movement sleep homeostatic cascade. J Neurochem. 116:260–272.

Katz LC. 1987. Local circuitry of identified projection neurons in cat visual cortex brain slices. J Neurosci. 7:1223–1249.

Kawaguchi Y, Kondo S. 2002. Parvalbumin, somatostatin and cholecystokinin as chemical markers for specific GABAergic interneuron types in the rat frontal cortex. J Neurocytol. 31:277–287.

Kerr MI, Wall MJ, Richardson MJ. 2013. Adenosine a1-receptor activation mediates the developmental shift at layer-5 pyramidal-cell synapses and is a determinant of mature synaptic strength. J Physiol. 591:3371–3380.

Killgore WD. 2010. Effects of sleep deprivation on cognition. Prog Brain Res. 185:105–129.

Klyuch BP, Dale N, Wall MJ. 2012. Deletion of ecto-5′-nucleotidase (cd73) reveals direct action potential-dependent adenosine release. J Neurosci. 32:3842–3847.

Klyuch BP, Richardson MJ, Dale N, Wall MJ. 2011. The dynamics of single spike-evoked adenosine release in the cerebellum. J Physiol. 589:283–295.

Kruglikov I, Rudy B. 2008. Perisomatic GABA release and thalamocortical integration onto neocortical excitatory cells are regulated by neuromodulators. Neuron. 58:911–924.

Larsen DD, Callaway EM. 2006. Development of layer-specific axonal arborizations in mouse primary somatosensory cortex. J Comp Neurol. 494:398–414.

Larsen DD, Wickersham IR, Callaway EM. 2007. Retrograde tracing with recombinant rabies virus reveals correlations between projection targets and dendritic architecture in layer 5 of mouse barrel cortex. Front Neural Circuits. 1:5.

Le Be JV, Silberberg G, Wang Y, Markram H. 2007. Morphological, electrophysiological, and synaptic properties of corticocallosal

pyramidal cells in the neonatal rat neocortex. Cereb Cortex. 17:2204–2213.
Li Y, Fan S, Yan J, Li B, Chen F, Xia J, Yu Z, Hu Z. 2011. Adenosine modulates the excitability of layer II stellate neurons in entorhinal cortex through a1 receptors. Hippocampus. 21:265–280.
Liang BT, Jacobson KA. 1999. Adenosine and ischemic preconditioning. Curr Pharm Des. 5:1029–1041.
Little JP, Carter AG. 2012. Subcellular synaptic connectivity of layer 2 pyramidal neurons in the medial prefrontal cortex. J Neurosci. 32:12808–12819.
Lu G, Zhou QX, Kang S, Li QL, Zhao LC, Chen JD, Sun JF, Cao J, Wang YJ, Chen J et al. 2010. Chronic morphine treatment impaired hippocampal long-term potentiation and spatial memory via accumulation of extracellular adenosine acting on adenosine a1 receptors. J Neurosci. 30:5058–5070.
Mander BA, Rao V, Lu B, Saletin JM, Lindquist JR, Ancoli-Israel S, Jagust W, Walker MP. 2013. Prefrontal atrophy, disrupted NREM slow waves and impaired hippocampal-dependent memory in aging. Nat Neurosci. 16:357–364.
Manns ID, Sakmann B, Brecht M. 2004. Sub- and suprathreshold receptive field properties of pyramidal neurones in layers 5a and 5b of rat somatosensory barrel cortex. J Physiol. 556:601–622.
Marx M, Feldmeyer D. 2013. Morphology and physiology of excitatory neurons in layer 6b of the somatosensory rat barrel cortex. Cereb Cortex. 23:2803–2817.
Marx M, Gunter RH, Hucko W, Radnikow G, Feldmeyer D. 2012. Improved biocytin labeling and neuronal 3D reconstruction. Nat Protoc. 7:394–407.
McCormick DA, Williamson A. 1989. Convergence and divergence of neurotransmitter action in human cerebral cortex. Proc Natl Acad Sci USA. 86:8098–8102.
Molnar Z, Cheung AF. 2006. Towards the classification of subpopulations of layer V pyramidal projection neurons. Neurosci Res. 55:105–115.
Muzur A, Pace-Schott EF, Hobson JA. 2002. The prefrontal cortex in sleep. Trends Cogn Sci. 6:475–481.
Oberlaender M, De Kock CP, Bruno RM, Ramirez A, Meyer HS, Dercksen VJ, Helmstaedter M, Sakmann B. 2012. Cell type-specific three-dimensional structure of thalamocortical circuits in a column of rat vibrissal cortex. Cereb Cortex. 22:2375–2391.
Oken BS, Salinsky MC, Elsas SM. 2006. Vigilance, alertness, or sustained attention: physiological basis and measurement. Clin Neurophysiol. 117:1885–1901.
Otsuka T, Kawaguchi Y. 2008. Firing-pattern-dependent specificity of cortical excitatory feed-forward subnetworks. J Neurosci. 28:11186–11195.
Paxinos G, Watson C. 2005. The rat brain in stereotaxic coordinates. San Diego (CA): Academic Press.
Pichon F, Nikonenko I, Kraftsik R, Welker E. 2012. Intracortical connectivity of layer VI pyramidal neurons in the somatosensory cortex of normal and barrelless mice. Eur J Neurosci. 35:855–869.
Poorthuis RB, Bloem B, Schak B, Wester J, De Kock CP, Mansvelder HD. 2013. Layer-specific modulation of the prefrontal cortex by nicotinic acetylcholine receptors. Cereb Cortex. 21:148–161.
Porkka-Heiskanen T, Strecker RE, Mccarley RW. 2000. Brain site-specificity of extracellular adenosine concentration changes during sleep deprivation and spontaneous sleep: an in vivo microdialysis study. Neuroscience. 99:507–517.
Porkka-Heiskanen T, Strecker RE, Thakkar M, Bjorkum AA, Greene RW, Mccarley RW. 1997. Adenosine: a mediator of the sleep-inducing effects of prolonged wakefulness. Science. 276:1265–1268.
Prince DA, Stevens CF. 1992. Adenosine decreases neurotransmitter release at central synapses. Proc Natl Acad Sci USA. 89:8586–8590.
Radnikow G, Günter RH, Marx M, Feldmeyer D. 2012. Morpho-functional mapping of cortical networks in brain slice preparations using paired electrophysiological recordings. In: Fellin T, Halassa MM, editors. Neural Network Analysis. 1st ed. Berlin (Germany): Springer. pp. 405–431.
Rainnie DG, Grunze HC, Mccarley RW, Greene RW. 1994. Adenosine inhibition of mesopontine cholinergic neurons: implications for EEG arousal. Science. 263:689–692.
Rebola N, Lujan R, Cunha RA, Mulle C. 2008. Adenosine a2a receptors are essential for long-term potentiation of NMDA-EPSPs at hippocampal mossy fiber synapses. Neuron. 57:121–134.
Ruby CL, Adams CA, Knight EJ, Nam HW, Choi DS. 2010. An essential role for adenosine signaling in alcohol abuse. Curr Drug Abuse Rev. 3:163–174.
Schmitt LI, Sims RE, Dale N, Haydon PG. 2012. Wakefulness affects synaptic and network activity by increasing extracellular astrocyte-derived adenosine. J Neurosci. 32:4417–4425.
Segal M. 1982. Intracellular analysis of a postsynaptic action of adenosine in the rat hippocampus. Eur J Pharmacol. 79:193–199.
Seong HJ, Carter AG. 2012. D1 receptor modulation of action potential firing in a subpopulation of layer 5 pyramidal neurons in the prefrontal cortex. J Neurosci. 32:10516–10521.
Thomson AM. 2010. Neocortical layer 6, a review. Front Neuroanat. 4:13.
Thompson SM, Haas HL, Gahwiler BH. 1992. Comparison of the actions of adenosine at pre- and postsynaptic receptors in the rat hippocampus in vitro. J Physiol. 451:347–363.
Thorndike RL. 1953. Who belongs in the family? Psychometrika. 18:267–276.
Tömböl T. 1984. Layer VI cells. In: Peters A, Jones EG, editors. Cerebral cortex. 1st ed. London (UK): Plenum Press. pp. 479–510.
Van Aerde KI, Feldmeyer D. 2015. Morphological and physiological characterisation of pyramidal neuron subtypes in rat medial prefrontal cortex. Cereb Cortex. 25:788–805.
Van Aerde KI, Mann EO, Canto CB, Heistek TS, Linkenkaer-Hansen K, Van Der Roest M, Mulder AB, Paulsen O, Brussaard AB, Mansvelder HD. 2009. Flexible spike timing of layer 5 neurons during dynamic beta-oscillation shifts in rat prefrontal cortex. J Physiol. Pt21:5177–5196.
Van Brederode JF, Snyder GL. 1992. A comparison of the electrophysiological properties of morphologically identified cells in layers 5b and 6 of the rat neocortex. Neuroscience. 50:315–337.
Van Der Werf YD, Altena E, Schoonheim MM, Sanz-Arigita EJ, Vis JC, De Rijke W, Van Someren EJ. 2009. Sleep benefits subsequent hippocampal functioning. Nat Neurosci. 12:122–123.
Van Der Werf YD, Witter MP, Groenewegen HJ. 2002. The intralaminar and midline nuclei of the thalamus. Anatomical and functional evidence for participation in processes of arousal and awareness. Brain Res Brain Res Rev. 39:107–140.
Van Dort CJ, Baghdoyan HA, Lydic R. 2009. Adenosine a(1) and a(2a) receptors in mouse prefrontal cortex modulate acetylcholine release and behavioral arousal. J Neurosci. 29:871–881.
Van Eden CG, Uylings HB. 1985. Cytoarchitectonic development of the prefrontal cortex in the rat. J Comp Neurol. 241:253–267.
Vertes RP, Hoover WB, Szigeti-Buck K, Leranth C. 2007. Nucleus reuniens of the midline thalamus: link between the medial prefrontal cortex and the hippocampus. Brain Res Bull. 71:601–609.
Walker MP. 2008. Cognitive consequences of sleep and sleep loss. Sleep Med. 9(Suppl 1):S29–S34.
Wall MJ, Atterbury A, Dale N. 2007. Control of basal extracellular adenosine concentration in rat cerebellum. J Physiol. 582: 137–151.
Wang XJ. 1999. Synaptic basis of cortical persistent activity: the importance of NMDA receptors to working memory. J Neurosci. 19:9587–9603.
Wang Y, Markram H, Goodman PH, Berger TK, Ma J, Goldman-Rakic PS. 2006. Heterogeneity in the pyramidal network of the medial prefrontal cortex. Nat Neurosci. 9:534–542.
Yang CR, Seamans JK, Gorelova N. 1996. Electrophysiological and morphological properties of layers V–VI principal pyramidal cells in rat prefrontal cortex in vitro. J Neurosci. 16:1904–1921.
Yellon DM, Downey JM. 2003. Preconditioning the myocardium: from cellular physiology to clinical cardiology. Physiol Rev. 83: 1113–1151.
Yoon KW, Rothman SM. 1991. Adenosine inhibits excitatory but not inhibitory synaptic transmission in the hippocampus. J Neurosci. 11:1375–1380.